# PARAMETRIC ANALYSIS AND SIMULATION OF A TUGBOAT PROPELLER BLADE

**BY**

**OKONI, Demas Alfred**
**MENG/SEET/2017/6933**

**DEPARTMENT OF MECHANICAL ENGINEERING**

**FEDERAL UNIVERSITY OF TECHNOLOGY**

**MINNA**

**JANUARY 2022**

# PARAMETRIC ANALYSIS AND SIMULATION OF A TUGBOAT PROPELLER BLADE

**BY**

**OKONI, Demas Alfred**
**MENG/SEET/2017/6933**

**A THESIS SUBMITTED TO THE POSTGRADUATE SCHOOL, FEDERAL UNIVERSITY OF TECHNOLOGY, MINNA, NIGERIA IN PARTIAL FULFILMENT OF THE REQUIREMENTS FOR THE AWARD OF MASTER OF ENGINEERING IN MECHANICAL (THERMOFLUID AND POWER PLANT OPTION)**

**JANUARY 2022**

## ABSTRACT

The parametric analysis of a tugboat propeller blade was carried out with solidworks computer aided simulation software. The aim is to achieve vibration and noise mitigation as well as performance improvement of the propulsion system by varying the number of propeller blade to ascertain minimum allowable pressure on the propulsion system. To determine the magnitude of stiffness assumed in the dynamic part of the propulsion system, modeling the propulsion system as an elastic spring and perform vibration analysis-static and dynamic analysis on the propulsion system, and to analyze the fluid dynamics on the structure which may in turn have impact on the propulsion system. For this study, Concept design and vibration analysis were adopted with external militating factor like the mass of the tug (5000 tons), the viscosity of the water, the power of the propeller engine,$2^{nd}$ order vertical moment, of the propeller engine and experimental modal parameters (natural frequency, propeller blade radius, number of propeller blade, length of shaft). In consideration, the research finding shows that the pressure build-up ($2.14 \times 10^8$) around the propeller with six blades is high compared to that of with three blades which is ($1.27 \times 10^8$) The performance of the propulsion system improves, but the pressure on the propeller resulting to increased pressure build-up on the blade may result in possible failing. Thus for a tugboat of mass 5000 tons the research finding shows that an RPM of 49.7785rad/sec for the propeller blade is feasible. The research however recommends that in operation, if the propeller RPM is higher than the number of propeller blade, it ensures that the torque required to spin the propeller is reduced. The length and diameter obtained be considered in other to increase the stiffness.

## TABLE OF CONTENTS

## LIST OF APPENDICES



## LIST OF TABLES

## LIST OF FIGURES

## ABBREVIATION, GLOSSARIES AND SYMBOLS

| Symbol | Description | Unit |
|---|---|---|
| k | Stiffness | N/m |
| ω | Excitation frequency | Rev/sec |
| $\omega/\omega_n$ | Natural frequency | - |
| n | Number of propeller | - |

| | | |
|---|---|---|
| RPM | Propeller rate of rotation | Rev/sec |
| $\zeta$ | Damping coefficient | kNs/m |
| $M_{2v}$ | 2nd Order vertical moment | N-m |
| PRU | Power Related Unbalance | N-m |
| P | Engine power | kW |
| $K_1$ | Stiffness of propeller shaft | N/m |
| $K_2$ | Stiffness of line-shaft | N/m |
| $K_3$ | Stiffness of thrust bearing elements and engine foundation | N/m |
| $M_1$ | Lumped mass at the propeller | kg |
| $M_2$ | Lumped mass at propeller shaft/line shaft coupling | kg |
| $M_3$ | Lumped mass at thrust bearing | kg |
| $A$ | Shaft cross-sectional area | $m^2$ |
| m | Lumped mass | kg |
| d | Thickness of the shaft | m |
| G | Modulus rigidity | GPa |
| F | Force acting on the surface of the shaft | N |
| D | Diameter of the shaft | m |
| y | Total deflection | m |
| N | Number of turns of the shaft | - |
| $R_T$ | Total resistance | N |
| $C_T$ | Total resistance coefficient | - |
| $\rho_w$ | Water density | $Kg/m^3$ |
| $S_w$ | Wetted surface area of the underwater hull | $m^2$ |
| $V_s$ | Maximum speed of hull | m/s |
| $C_w$ | Wake making resistance coefficient | - |

| | | |
|---|---|---|
| $C_F$ | Frictional resistance coefficient | - |
| $C_A$ | Incremental resistance coefficient | - |
| $C_v$ | Viscous resistance coefficient | - |
| $C_{AA}$ | Air resistance coefficient | - |
| ν | Kinematic viscosity of water | $m^2/s$ |
| $KC_F$ | normal (viscous pressure drag) Component of viscous resistance | |
| L | Length of the Ship | m |
| $L_{PP}$ | Length Between Perpendiculars | m |
| $\eta_D$ | Delivered efficiency of propeller | - |
| $\eta_H$ | Hull efficiency | - |
| $\eta_o$ | Propeller open water efficiency | - |
| $P_E$ | Effective power | kW |
| t | Thrust deduction fraction | |
| $P_D$ | Delivered power of propeller | kW |
| $P_P$ | Propulsion power | kW |
| $\eta_B$ | Behind propeller efficiency | - |
| $P_S$ | shaft power | kW |
| $P_B$ | Brake power | kW |
| $V_A$ | Advance velocity | m/s |
| $B$ | waterline breadth of the hull | m |
| w | Taylor's wake fraction | - |
| $\delta_{opt}$ | Optimum diameter | m |
| $A_o$ | Blade area (disk area) | $m^2$ |
| $A_P$ | Projected area of the blade | $m^2$ |

| | | |
|---|---|---|
| $A_E$ | Expanded area of the blade | $m^2$ |
| $A_D$ | Developed area of the blade | $m^2$ |
| p | Pitch of the propeller blade | m |
| T | Thrust of the propeller blade | N |
| $P_T$ | Thrust Power of the propeller blade | kW |
| $Q_B$ | Engine Shaft Torque | Nm |
| $t_o$ | Maximum Blade Thickness | m |
| W | Weight of the propeller blade | N |
| $B_{tf}$ | Blade Thickness Fraction | - |
| ς | Blade Area Fraction | - |
| Y | Specific Weight of Blade Material | $N/m^3$ |
| R | Propeller Tip Radius | m |
| $I_P$ | Polar Moment of Inertia of all Blades | $Nm^2$ |
| σ | Stress | $N/m^2$ |
| F | Force on the propeller blade | N |
| $A_O$ | Disk area of propeller blade | $m^2$ |
| ω | Angular Speed | rad/s |
| $L_{wl}$ | waterline length of the ship hull | m |
| Z | Number of Blades | - |
| $F_n$ | Froude number | - |
| Δ | Displacement of the hull | m |
| T | Draught amidships | m |
| $C_B$ | Block coefficient | - |
| $R_n$ | Reynolds number | |
| $B_P$ | Power coefficient | - |

# CHAPTER ONE

# INTRODUCTION

## 1.1 Background of study

It is believed that in operation, mechanical structures are subjected to dynamic forces which cause vibrations and if not well managed or mitigated against the structure, failure may take place. Because vibration can be total vibration of the entire structure or local which is vibration of selective structural components or a mix of both, it has to be considered in a comprehensive way. Proper levels of vibration need to be maintained to limit an increased rate of fatigue failure in structural members and the malfunction of machinery and equipment.

Personnel task performance is a key component of operational safety, and a critical component of task performance is habitability, which includes noise and whole-body vibration. Designing for performance and habitability goals allows for improvement of productivity, morale, safety, and comfort, and it reduces potential risk of fatigue and human error.

Noise and vibration performance goals are best achieved if noise and vibration analysis are carried out and mitigation are considered in early design stages. The cost of correcting a potential noise and/or vibration issue can be up to ten (10) times as expensive after construction than if incorporated into the design from preliminary design stage (ABS, 2018).

The word Propulsion originated from the Latin words pro, which means before or forward, and pellere, which means to drive. Propulsion systems comprise of all the components used in generating power, transmitting these power to the propeller via a shaft and reduction gear, which in turn converts this power to thrust used in moving a vessel forward. Ship propulsion is not only restricted to just moving vessel forward

against forces such as air drag, friction, towing resistance etc., but is also responsible for stopping, maneuvering of the vessel and keeping it in a static position against water current when required. A tug boat is a small but very powerful vessel used in towing (pulling) or tugging bigger vessels that cannot move by themselves or are not self-propelled like some barges. Tug boats can also be used as fire fighters, ice breakers etc. the strength of a tug boat and its ability to maneuver effectively depends solely on the propulsion system installed (Nitonye *et al.*, 2017). There are different types of propulsion system for marine operation. Diesel electric propulsion system is one of the propulsion that has configuration that is fitted with the bow and aft thrusters, and is often mounted with one up to eight azimuth thrusters. The bow and aft thrusters are electrically driven. Although the impacts of these ships on the whole maritime industry is most times been neglected, but their value is mostly felt in maneuvering during bad weather conditions and during vessel breakdown etc. Most important factor of the propulsion system is the interaction between the propeller and the nozzle with the hull. It is also believed that this research work will be significant in terms of designing tugboats with low fuel consumption and operating cost.

### 1.2 Statement of the Research Problem

The importance of tugboat cannot be over emphasized in a region like the Niger Delta with vast coastal lines. The effectiveness of a tugboat is characterized by its ability to tow and maneuver easily, which is a major concern in the marine industry. Excessive vibration and noise has done so many damages to the propulsion system by causing crew discomfort and inefficient performance of the tugboat. This has also led to causing potential damage to the system, increased rate of fatigue in structure members and also malfunctioning of materials /equipment. However, the aftermath effect of increased

negative pressure on the propeller blade of the propulsion system have caused tugging effort being futile, leading to time wastage, accrued cost and possible loss of life (Geertsma *et al*., 2017).

There is so much demand for more efficient propulsion system in a tugboat due to increased maritime operations with the view of improving crew comfort and performance by imposing limitation and restriction to vibration and noise limit. Appropriate vibration levels can enhance operational safety by improving task performance, habitability, proper functioning of sensitive equipment, such as sensors and modern monitoring technologies as well as whole-body structural integrity at sea.It is worth therefore to investigate performance characteristics of the propulsion system that will ensure optimal performance improvement of the propulsion against possible issues that may prompt failure.

### 1.3 Justification of the Study

This project involves Optimum Performance Analysis of a Tugboat Propulsion System using solidworks engineering CAD software to aid the analysis. The tugboat propulsion is a model to be able to tug a ship of minimum mass of 5000 tons. The vibration of propulsion system might occur due to the low magnitude of skew angle. These optimum parameters will be determined for propeller with 3, 4, 5 and 6 blades.

### 1.4 Aim and Objectives of the Study

#### Aim

The aim of this project is to evaluate the performance of propulsion system of a tugboat through the analysis of the mechanical structures with a view to getting the desired

tugboat dimensions. To achieve the aim, the study is guided with the following specific objectives to:

(1) Carry out design analysis of effective power, tug resistance and power of a tugboat propulsion system

(2) Carry out simulation and parametric analysis of various blades of propeller.

(3) Examine the vibration effect of propulsion where different numbers of blades are used.

(4) Estimate properties of a tugboat that will enhance effectiveness of propulsion.

## 1.5 Significance of the Study

- The findings of this study would help in predicting possible issues/factors associated with vibration of a propulsion system.
- It will also serve as a reference for further research(es) for propulsion system performance improvement in tugboat.
- Finally, it is expected to contribute to the body of knowledge in the area of the dynamic part of propeller performance improvement.

## 1.6 Scope of the Work

This work is limited to the design and optimum performance analysis of a tugboat propulsion system capable of transporting a ship of a maximum load of about 5000 tons ($4.53 \times 10^6$kg) to any suitable direction, mitigating possible failure due to vibration. The forcing function Modal analysis and Finite Element Analysis is performed using Excel Sheet and the solidworks modeling and simulation tool of analysis defined on the structural model of the mass, the damping and the stiffness of the propeller shaft with the aim to acquire information on the local vibration response which depends on the type of structural elements to which the analysis is oriented.

# CHAPTER TWO

# LITERATURE REVIEW

## 2.1 Early Development

Devises for bating ships have been in existence for a very long time. Man initially made use of his head and hack, with time man began to develop ideas on how to produce a device capable of pushing or towing ships over short distances without using human effort which are usually employed aided by a tow rope to bat ships or heavy trucks or tankers. The advent of the propulsion system was able to improve the process but was without its own challenges as observed.

Kumar *et al.*, (2019), in their work on the mechanical behavior of propulsion system considering the designed load and boundary conditions adopting finite element method. The finite element method was adopted to estimate the possible stiffness and stress imposed on the system during operation and as a result of external load imposed on the system it also aided in determining the buckling load by monitoring stress, state and energy absorbed in component for prediction of performance worthiness. The plastic deformation value obtained was used to estimate the value of additional stress if imposed on the system will result to possible issues of system failure.

Scondipon *et al.,* (2002) performed a comparative analysis on multiple parameter damped mechanical systems, with basic issues as regards damping in linear dynamic systems and coming up with viable methods for analysis and sorting of generally damped linear systems in consideration. This study used the vibrating systems as a case study. The concept design approach was adopted aided by parametric analysis and the result of the analysis showed that regardless of the nature of the damper proportional damping can exist. The result also gave impetus towards understanding damping mechanisms in

general mechanical systems. The researcher recommended both damping mechanisms should be adopted on the ground of operational definitions.

According to Herman (2001) in his review on the test procedure and system identification principles of modal analysis, considering the observable challenges encountered by engineers while performing parametric analysis on structures. The study enquires into the possible phenomenon like measurement principles, estimation of parameter, test definitions and instrumentation. The review shows that if a mechanical structure is analyzed as a lump sum only will limit the researcher's intent if the boundary conditions are neglected. Thus, the researcher recommends that a more detailing approach is adopted to aid the parametric analysis, such approach as finite element analysis.

Saqlain and He (2007) worked on optimization and sizing for propulsion system of Liquid Rocket Using Genetic Algorithm to help to automate part of the design process with this effort directed towards developing a propulsion system design strategy for liquid rocket to optimize take-off mass, satisfying the mission range under the constraint of axial overload. This process was accomplished by using Genetic Algorithm as optimizer.

Also is the work of veloso *et al*., (2009), where they enquired into the mechanism of tugboat propulsion adopting a vehicle (tow van) which prototype propulsion system of a tugboat. The result of the analysis shows that the failure actually takes place at the bumper fixation point of the vehicle where the mooring rope was attached; during the test on increasing the mass of the tow observable crack was created which stems high causing possible fracture of the component. For detailed analysis the Finite element analysis centered on quasi-experimental approach and durability test analysis was adopted, and this gave a clear picture of possible issues of failure in the system.

Ravikant and Mukesh (2013), worked on parametric analysis of drive shaft using finite element method, considering the design essence of the drive shaft to set other shaft in motion about its axis. The solidworks simulation software and ANSYS workbench was employed to perform a finite element analysis on the shaft with the inherent frequencies and vibration mode shapes with their respective deformation in view. The result of the analysis shows the stress point and possible point of failures of the shaft and also how frequency variation inspires vibration of the system was explained by the modal analysis of the shaft.

The study by Franklin and Tecnavin (2013) investigated the possible issues of vibration and failure in propulsion system of selected mechanical structures. The shaft designed software (TORAN) was adopted for the study, performing basic vibration analysis and estimating the possible issues that may result to the failure of the entire component part of the propulsion system. The result of the study was presented as a benchmark for consideration when selecting the components of a propulsion system.

Soria *et al..,* (2012), worked on Operational Parametric Analysis and the performance assessment of vehicle suspension systems considering two suspension architectures equipping the same car type. Such systems included a semi-active commercial system and latter a novel prototypic active system. Parametric Analysis was adopted for the assessment of suspension performance, of the vehicle suspension system considering the impact of the different road profile and frequency vibration on the vibration of the system in view. On comparing the rest result considering the suspension types the prototypic active system shows more viability than the commercial system.

Tomas *et al.,* (2012), in their study on the modal analysis using the ANSYS Workbench environment, using the structural grid tool to calculate the dynamic response of the system to a surface of contact. The study also brings to bear the challenges on the system

as a result of the issue of preload parametric analysis and how to mitigate this problem, especially the nodal problem most times overlooked by the numerical or mathematical models when adopted.

Qianwen *et al.,* (2012), worked on the dynamics analytical theory and numerical simulation of the propulsion shafting considering the variation in the displacement and rotation angle caused by coupled torsional-longitudinal vibration of the system was varied at different sequences, the research result put up a recommendation on how to mitigate possible issues of coupled torsional-longitudinal vibration on the propulsion shafting.

## 2.2 Recent Developments of Tugboat Propulsion System

Throughout 1990s and 2000$^{th}$ advancements were made to improve tugboat propulsion mechanisms. The recent tugboat propulsion innovation is the Carousel Tug, winner of the maritime innovation award in Dutch maritime. This concept allows the tug to operate from angles which are not otherwise achievable and thereby utilize the hull in a completely different manner for both braking and steering when escorting. In the Carousel tug design, the hull is rotated in line with the towing wire from a fixed point which allows the towing wire to rotate freely around the hull. One advantage of this system is that the tow point moves to align with the direction of the pull. The thrust to power ratio is enhanced to mitigate the possible vibration effect on the propeller when approached by water which enters the propeller nozzle in a linear configuration and exist the nozzle in the same way.

Srimanthula *et al.,* (2013), worked on the reduction of vibration in mechanical structure incorporating passive damping and viscoelastic damping materials which help to dissipating vibration strain energy in the form of heat energy. These materials provide

the system with high possibility of high damping. To aid this study the model of a particular shaft is taken and analyzed using ANSYS. The structural analysis was performed to investigate the strength of the shaft and to compare the results for the materials. Modal analysis was also done on the shaft to determine mode shapes and to find their frequencies.

Adil and Fulgence (2014) in the work; “Fluid structure interaction effects on the propulsion of a flexible composite monofin” proposed that finite element method be adopted to analyze the propulsive efficiency of a swimming fin by using the fluid-structure interaction model to investigate the effect of added mass on the natural frequencies of the fin oscillating in a compressible fluid. It has been shown that considering the added mass effects in water environment, the natural frequencies of the fin was found to decrease.

Lech, (2014) worked on the vibrations Resonance Estimation in Marine Structure on the ground that the Dynamic analyses of a marine structure are vital during design process as well as during exploitation. This study adopted two parts of vibrations calculations defined upon the natural vibrations frequencies and modes are determined and forced vibrations analysis, where the natural vibrations gives information on the possibility (e.g at which main engine speed) of dangerous vibrations amplitudes (resonances threat) that gives exact values of vibrations amplitudes as a result of forced vibrations analysis. Confidence level (error value) of forced vibration calculations is much lower in comparison to uncertainty of natural vibration analysis. The study also analyses the characteristics of hybrid propulsion shafting and builds mathematical models and vibration equations of shafting using the lumped parameter method. Model result was validated by testing results conducted on double diesel propulsion shafting bench. Mathematical model and model-building methods of shafting were correct.

Amirhossein *et al..,* (2015), worked on multidisciplinary Design Optimization and analysis of Hydrazine Monopropellant Propulsion System, considering the following optimization factors-tank pressure, catalyst bed length and diameter, catalyst bed pressure, and nozzle geometry directed towards the optimization propulsion system total mass which includes, mass of the propellant and the mass of the integral part design of the propulsion system.

Baroudia *et al..,* (2015), worked on determining the propulsive efficiency of a swimming fin. For this, they used a fluid-structure interaction model, taking into account the isentropic character of each layer of the fin. The numerical solution of the coupled problem has been performed using finite element method.

Hassan and Hamid, (2015), worked on model selection and dynamic analysis of marine structure propulsion system using finite element models. The researchers in the study considered the experimental modal parameters such as the natural frequencies of the shaft line, which is deduced by running vibration testing with the aid of designated software to ensure that possible environmental parameters and boundary condition are put into place. This study shows that the length of the marine structure, the diameter and thickness play a vital role in the quest for vibration mitigation. The researchers recommended that during concept design phase, reliable diameter and thickness should be ensured to compensate for the length.

In a report by Sen and Minoru (2015) on Torsional Vibration Characteristics of Marine Diesel Propulsion System Installed with the Highly-Elastic Rubber Coupling, the researchers came up with a practical calculation method for torsional vibration analysis-modal analysis with all parameters and boundary condition in place. The study findings showed proximity with natural observation and the modeled results.

Nengqi *et al..,* **(**2016), studied the vibration of Marine Diesel-Electric Hybrid Propulsion System. Dynamic analysis of marine structures is one of the most important during process as well as during exploitation. Typically, two parts of vibrations calculations were performed considering the estimation of dynamic characteristics and possibility for characteristics fluctuation in practice, with the objective centered on estimating the natural vibrating frequency of the structure. The utility of relatively simple models, with low degree of freedom number, was discussed with the quest to identify torsional vibration. The gains and ills of subcritical and supercritical design of marine propulsion system were discussed.

## 2.3 Knowledge gap based on literature review

The above review reveals that the effect of this knowledge area has not been treated extensively to the entire propulsion system analysis in the previous work and the environmental or external factors such as the viscosity of the water, the average pressure of the sea states, etc with the use of industrial based software for analysis (e.g Solidworks, ANSYS etc).These previous works talked about part of the propulsion system.

This project involves parametric analysis and simulation of a propeller blade used in tugboat propulsion system using solidworks engineering CAD software to aid the analysis. The tugboat propulsion is a model to be able to tug a ship of maximum mass of 5000 tons ($4.53 \times 10^6$kg).

## 2.4 Design Factors Consideration

In Tugboat vibrations, four elements of importance are normally considered. They are excitation, stiffness, frequency ratio, and damping.

### 2.4.1 Excitation problem

This is said to occur when the frequency of vibration exceeds the threshold frequency. The propulsion system has been identified as a major source of excitation in a vessel, with the propeller and the engine a key accomplist. It is appropriate that the principal vibration exciting sources be addressed first since with high excitation levels excessive vibration can occur almost independently of the system structural characteristics.

### 2.4.2 Stiffness value determination

Stiffness k is defined as spring force per unit deflection. In general, stiffness is to be increased rather than decreased when variations in natural frequency are to be achieved by variations in stiffness. Stiffness can be altered by improper selection of the pitch and redefining the engine foundation.

### 2.4.3 Frequency ratio

Values of frequency ratio near unity should be avoided as $\omega/\omega_n = 1$ is the resonant condition**.** At resonance, the excitation is opposed only by damping. Note that $\omega/\omega_n$ can be varied by varying either excitation frequency $\omega$ or natural frequency $\omega_n$. In the case of propeller induced vibration of a propulsion system, the system can be said to be damped by changing the propeller RPM or its number of blades. $\omega_n$ is changed by changes in system mass and/or stiffness; increasing stiffness is the usual and preferred approach. If geometry is held constant, simply increasing the elastic modulus with a different material.

### 2.4.4 Damping evaluation

Damping, $\zeta$ of structural systems in general and of ships in particular, is small;

$\zeta << 1$. Increasing damping tend to reduce isolation at the higher frequencies. Therefore, except very near resonance, the vibratory amplitude is approximately damping independent. Furthermore, damping is difficult to increase significantly in systems such

as ships; ζ is, in general, the least effective of the four parameters available to the designer for implementing changes in ship vibratory characteristics.

## 2.5 Design Theory

A primary requirement of marine propeller material is of heat treatable and high strength used for structural members where performance is critical under compressive loading. Marine propellers are made from corrosion resistant as they are made operational directly in seawater which is a corrosion accelerator.

The materials used for making marine propeller are alloy of aluminum and stainless steel. Other popular materials are alloy of nickel and bronze which are relatively lighter than other materials and have higher strength. Aluminum alloys have been extensively considered for high performance propeller (Carlton, 2019).

Aluminum alloys are very good having good properties for testing propeller optimal for boat. For impact underwater object, the propeller usually fails instead of causing damage to shaft or seals. Its continual usage has been recommended (ABS, 2018) for conventional application and where a material evaluation program is not practical. The properties of aluminum are shown below (Seetharama *et al*., 2012).

Young's modulus E= 70000 MPa

Poisson's ratio =0.29

Mass density =2700 gm/cc

Damping co-efficient =0.03

In applications, aluminum appears to offer the blade designer the best opportunity to achieve the optimum weight-strength design (Kiam *et al*., 2014).

Parametric analysis further deals with the concept design approach, design process of the boat propeller, designs estimations (Force of the Tug, Thrust T, and Torque $Q_B$).

Solidworks 2018 software was used to determine the static and dynamic analysis of the Propeller blade. This standard propeller is skewed by 20°, has a Rake angle of 4.05° (Nturamato *et al*., 2018).

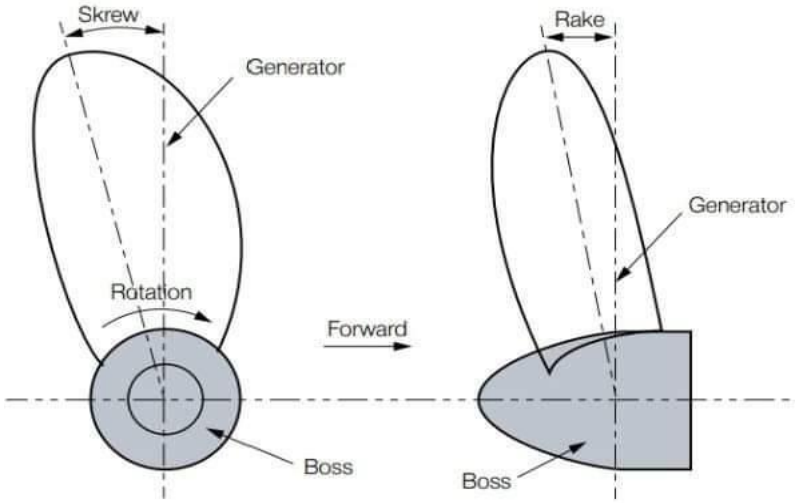


Figure 2.1 Skew and Rake angle (Nturamato *et al*., 2018)

Model design is where the process of avoiding vibration must begin. Here possible issues of failures can be mitigated (ABS,2018) if the vibration problems which is said to be repeatedly identified by experience are addressed, at the earliest design stage, ultimately serious problems, involving great cost in correction efforts, can be avoided.

**2.6 Excitation problem mitigating to Improve Propeller performance (Result of Second Order Vertical Moment prediction)**

Excitation mitigation in a propulsion system ensures that the Power Related Unbalance (PRU) value is less than 120 N-m/kW and more recommendation is made if it exceeds 220 N-m/kW at an acceptable level of $M_{2v}$ which is possible for the entire structure. Table 2.1 below shows the value of the Power Related Unbalance at which a propulsion system may have need for compensator (damper).In practical terms, PRU helps the engine designer to decide the course of action to be followed (i.e. it gives an idea if there is a need to add moment compensators or damper).

Table 2.1: Excitation Compensation Scale

| PRU | Need for Compensator |
|---|---|
| Below 120 | Not likely |
| 120-220 | Likely |
| Over 220 | Most likely |

Source: ABC, 2018

**NOTE:** The designer request the values of 2$^{nd}$ order vertical moment of the engine from the engine manufacturer. This is to avoid resonance from rising by resulting in vertical vibration of the hull girder.

# CHAPTER THREE

# MATERIALS AND METHODS

## 3.1 Materials

The materials used in this research analysis includes

i). Aluminum alloy

ii). Standard Graphs, Charts and Tables

iii). Mathematical and engineering formulas,

iv). Solidworks software 2018 version

## 3.2 Methods

The methodology used in this research is the analytical method. The materials listed above were used accordingly as stated below. Mathematical and engineering formulas, graphs and charts were also used in the design of the propulsion system for the tug boat at the end of the design Solidworks software 2018 version was then used for result validation and iterations.

i). 3, 4, 5 6 bladed propellers of standard are modeled on Solidworks software 2018 version.

ii). These standard propellers are skewed by 20°, has a Rake angle of 4.05° and a diameter determined.

iii) Propellers are modified according to rake angle

iv). Analytical calculations are done for thrust, pitch and thickness variation with radius

v). Meshing of these propeller models is carried out on Solidworks software 2018 version.

vi). Aluminum Alloy propellers are considered for Static and Dynamic analyses

vii). Static and Dynamic analyses of the propellers are carried out on Solidworks software 2018 version.

viii). Comparative study is done based on Pressure developed due to the propeller blades, Velocity of water distribution along the propeller blade,

Stresses developed within the propeller when subjected to a thrust.

### 3.3 Power Related Unbalance determination for proper propeller performance

Section 2.6 is necessary in the engine selection stage where PRU exceeds 220N-m/Kw. ABS, 2018 recommends that either engines selection is changed or moment compensators is installed. This is supplied by the engine manufacturer and once that is done, the PRU is calculated (see the equation below)

$$\text{PRU} = \frac{M_{2v}[N-m]}{EnginePowerP[KW]} \tag{3.1}$$

$$M_{2v}\,[\text{N-m}] = \text{PRU} \times P \tag{3.2}$$

where

$M_{2v}$= 2nd Order Vertical moment $M_{2v}$ [N-m] obtained from the manufacturer

PRU = Power Related Unbalance

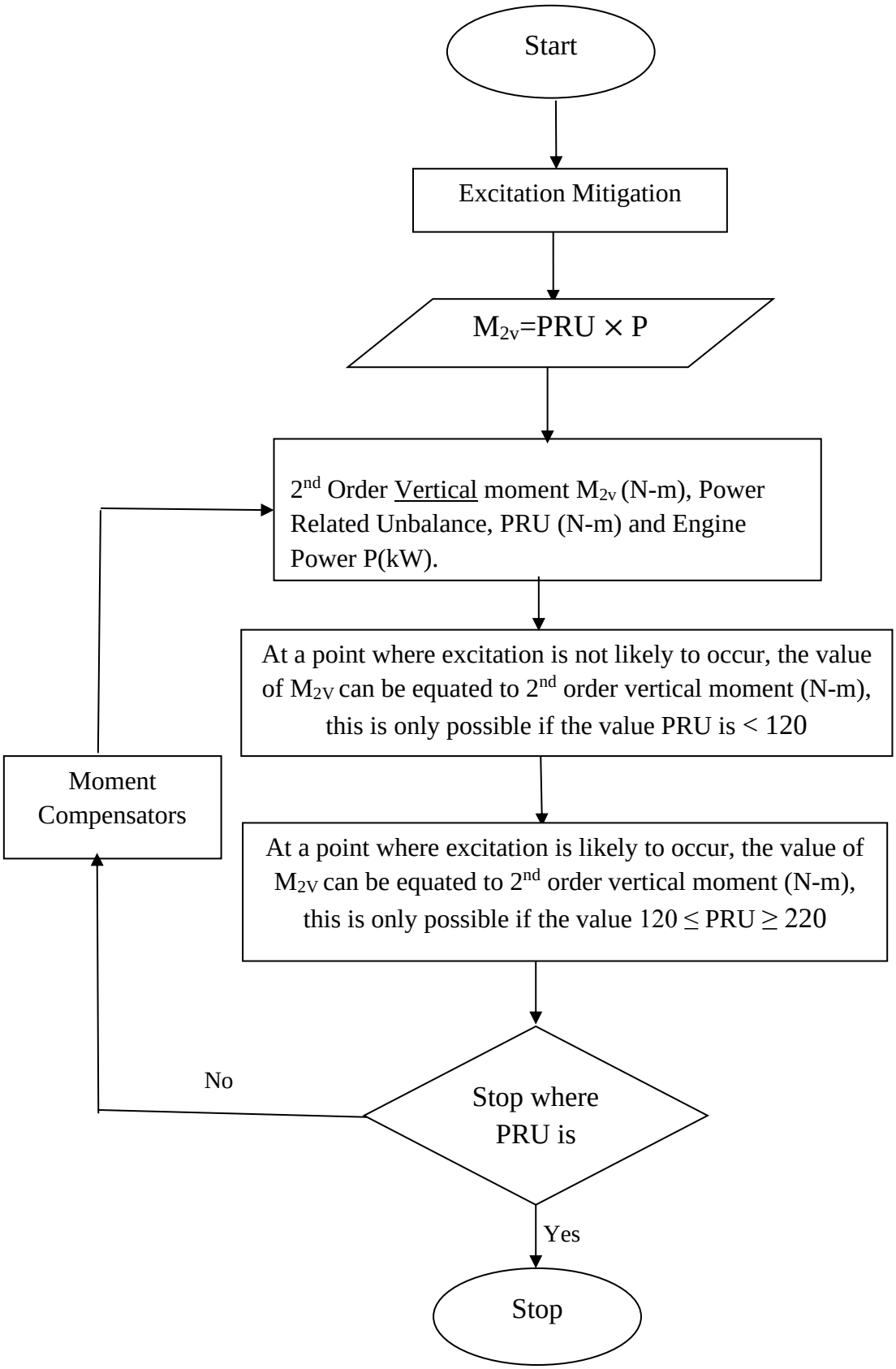


**Figure 3.1:** A process flowchart for excitation mitigation taking 2nd order vertical moment into considerations.

### 3.4 Stiffness Value Determination and Propeller Performance Improvement

The vibration of a system is seen to reduce if stiffness increases. The stiffness coefficient of feed bearing of some types of vessels is presented in Figure 3.2 below which the numerical value of stiffness can be determined. The tugboat shaft is a single line to the engine of the propeller and sensing the axial force from the propeller to the hull of the tug.

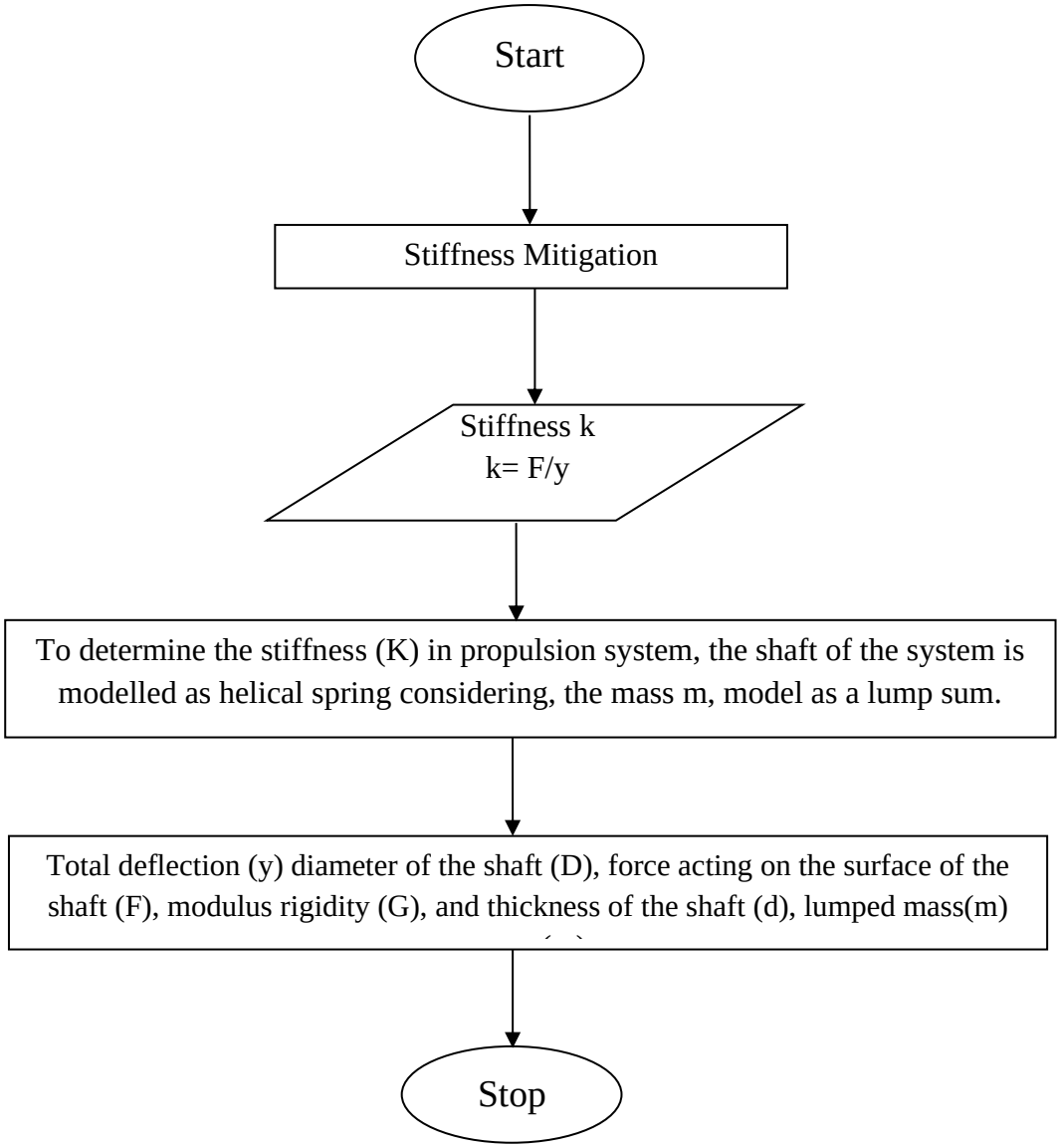


**Figure 3.2:** Process flow diagram for stiffness determination

The three mass model of Figure 3.3 below can be used for estimates of stiffness analysis. These three masses are considered the minimum number needed for estimating the propulsion system stiffness with reasonable accuracy (ABS, 2018).

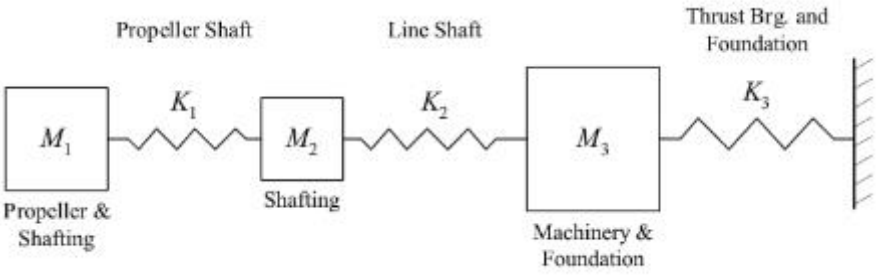


**Figure 3.3:** Mass Longitudinal Model of a Propulsion System (ABS, 2018).

where:

$M_1$ = lumped mass at the propeller in kg

$K_1$ = stiffness of propeller shaft in N/m, from propeller to coupling with line-shaft

= $AE/lp$

$A$ = shaft cross-sectional area in $m^2$

$M_2$ = lumped mass at propeller shaft/line shaft coupling in kg,

$K_2$ = stiffness of line-shaft in N/m,

$M_3$ = lumped mass at thrust bearing in kg,

$K_3$ = stiffness of thrust bearing elements and engine foundation in N/m

However, equation 3.3 below is also used to estimate the stiffness value at which excitation can be mitigated.

$$K = \frac{{d_S}^4 G}{{D_S}^3 N} = \frac{F}{y} \quad (3.3)$$

where:

y = Total deflection

F = Force acting on the surface of the shaft

$D_S$ = Diameter of the shaft

N = Number of turns of the shaft

$d_S$ = Thickness of the shaft

G = Modulus rigidity=79.3 GPa (www.engineeringtoolbox.com, 20/09/2020)

K= spring constant (stiffness)

Table 3.1 and 3.2 below illustrate the input values of the parameters needed to infer the stiffness of the propulsion system at which possible identified vibration can be mitigated.

**Table 3.1:** Input Parameters

| S/No | Parameters | Symbol | Units | Values |
|---|---|---|---|---|
| 1 | Diameter of the shaft | $D_S$ | m | 10.5 |
| 2 | Thickness of the shaft | $d_S$ | m | 16.0 |
| 3 | Number of turns of the shaft | N | - | 15.0 |
| 4 | Modulus of rigidity of the shaft | G | GPa | 79.0 |
| 5 | Mass of the tug | m | kg | $4.53 \times 10^6$ |

Source: Hassan and Hamid (2015)

**Table 3.2:** Propeller Shaft and Design Parameters

| Iteration | 1 | 2 | 3 | 4 | 5 |
|---|---|---|---|---|---|
| Diameter of Propeller Shaft(m) | 10.5 | 11 | 11.5 | 12 | 12.5 |
| Thickness of Propeller Shaft(m) | 16.0 | 17.0 | 18.0 | 19.0 | 20.0 |

Source: Hassan and Hamid (2015)

To determine the propulsion and performance of the system stiffness, the parameters were defined which will be needed for executing the simulations ahead. Firstly, an average mass of the tug was assumed to be 4530000kg bases that the force produced from the mass presses down by displacing water which is equivalent to the weight of the water pushing up, leaving the tugboat buoyant and also to provide support and services at offshore along with towing operations. This means M= ($4.53 \times 10^6$ kg) and it is equivalent to $45.3 \times 10^6$ N by weight.

### 3.5 Model Design approach

Using the acceptable results from above factors, may consistently be achieved with reasonable effort by the two of the four elements of importance like excitation and frequency ratio. The achievement in design of two objectives with regard to these elements has resulted in many successful ships:

i. Minimize dominant vibratory excitations, within the normal constraints imposed by other design variables, and
ii. Avoid resonances involving active participation of major subsystems in frequency ranges where the dominant excitations are strongest.

### 3.6 Design process and consideration for the boat propeller

Regarding the research objective to carry out design analysis of effective power, tug resistance and power of a tugboat propulsion system capable of propelling the tugboat for the various sea states to ascertain the maximum and minimum allowable pressure on the propulsion system, it is necessary to know the general specifications of boats, the specification of main propulsion engines, and the propellers specifications. Tugboat is categorized on the two groups' base on its size: it is either below or more than 30 GT.

This research will be focused on the propeller design for the first group. Statistics has shown that diameters of propellers are in range of 20 cm to 40 cm with the blade numbers mostly of 3-blades and some of them use 2-blades or 4-blades. Consequently, the boats have limitations regarding propulsion efficiency, as well as hull vibration; overheat main engine and high fuel consumption.

Initially, the boat hull form is selected as a representation of the boats population. Besides the resistance characteristics, the boat stern shape is also important factor for propeller design as the requirement of the propeller clearance. Figure 3.4 below presents the 3D geometries of four generated propeller characterized by the same EAR, $AE/A_O$, similar pitch ratio P/D and different blade numbers (Z= 3, 4, 5 and 6).

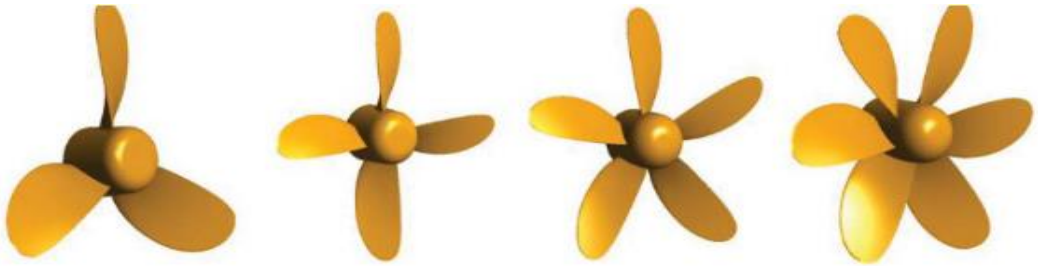

[a] 3-bladed | [b] 4-bladed | [c] 5-bladed | [d] 6-bladed

**Figure 3.4:** The three dimensional propeller design models

During design phase, some critical parameters like rake angle, skew angle, pitch angle and the hub diameter of propeller should be given. Hence, the three dimensional blades are drawn and the two dimensional propeller technical drawing can be generated. The three dimensional propeller design model can be seen in Figure 3.4 above. The technical drawing of the 4-bladed propeller is presented (see Appendix III)

## 3.7 Design Estimations/Analysis

The design estimations of the propulsion system of a propeller are analyzed in 8 sections as shown below.

### 3.7.1 Geometric specification of the Propeller

The initial design variable requirements of the propeller are;

1. Delivered power $P_D$
2. Propeller rate of rotation,
3. Speed of ship $V_S$,
4. Number of blades Z
5. Taylors wake fraction w

### 3.7.2 Tug Resistance Estimation

**(i) The total resistance $R_T$**

$$R_T = \frac{1}{2} \times C_T \times \rho_w \times S_w \times V_s^2 \quad (3.4)$$

where

$C_T$ = Total hull resistance coefficient (kg)

$\rho_w$ = Water density (kg/m$^3$)

$S_w$ = Wetted surface area of the underwater hull (m$^2$)

$V_s$ = Maximum speed of hull (m/s)

$$C_T = C_F + C_R + C_A. \quad (3.5)$$

But $C_R = K.C_F$.

By substitution,

$$C_T = C_F (1+K) + C_A \quad (3.6)$$

$C_A$ is equivalent to $C_W$ due to the fact that they are all Froude scaled

$$C_T = C_F (1+K) + C_w \quad (3.7)$$

But $C_V = C_F + C_R = = C_F (1+K)$

Hence

$$C_T = C_v + C_w$$

Where

$KC_F$ is the normal (viscous pressure drag) Component of viscous resistance

$C_A$ is the incremental resistance coefficient

$C_v$ is the viscous resistance coefficient

$C_F$ is the frictional resistance coefficient

$C_w$ is the wave making resistance coefficient

$t_1$ is the water temperature in degrees Celsius

K is the form factor which accounts for the effect of hull form on viscous resistance which is determined by

$$K = 19 \left(\frac{\nabla}{LBT_1} \times \frac{B}{L}\right)^2 \quad (3.8)$$

where; ∇ = displacement volume of the hull ship in a given draft, L = length of the hull ship, B = waterline breadth of the hull ship and $T_1$= the draught amid ship.

The incremental resistance coefficient $C_A$ is added in order to include the effect of the roughness of the surface of the ship. $C_A$ for model ship has very often been fixed at $C_A$ = 0.0004. However, experience has shown that $C_A$decreases with increasing boat size and the following roughness correction coefficient are proposed according to Harvald (1983). Table 3.3 shows the correction formula used to determine $C_A$ for a larger vessels (displacement more than 160000$t_1$).

**Table 3.3:** Roughness Correction Coefficient

| **Displacement(m)** | $C_A$ **Determinant** |
|---|---|
| ∇=1000 $t_1$ | $10^3 C_A$=0.6 |
| ∇=10000 $t_1$ | $10^3 C_A$= 0.4 |
| ∇=100000 $t_1$ | $10^3 C_A$= 0.0 |
| ∇=1000000 $t_1$ | $10^3 C_A$= -0.6 |

The frictional resistance coefficient $C_F$ is calculated by International Towing Tank Committee (ITTC'57) as follows:

$$C_F = \frac{0.075}{\lfloor LogRe - 2 \rfloor^2} \quad (3.9)$$

$$R_e = \text{Reynolds number} = \frac{LV_S}{\gamma} \quad (3.10)$$

**(ii) Analysis maximum hull speed, V**S

$V_S = 1.34 \times \sqrt{L}$ (3.11)

$$F_n = \frac{V_S}{\sqrt{Lg}} \quad (3.12)$$

where L = Waterline length of the hull ship

But $C_B = \frac{\nabla}{LBT_1}$ (3.13)

When the length, breadth and draught of the ship are equal then L = B = $T_1$.

Hence $C_B$ becomes $\frac{\nabla}{L^3}$ .

where ∇ = displacement volume of a ship in a given draft, B = waterline breadth of the hull ship and $T_1$= the draught amid ship.

For this study, block coefficient, $C_B$ is considered to be in the range 0.5 and 0.85 for constraint in optimization algorithm because the vessel is a bulk carrier. Hence the ship displacement is the weight of water that a ship pushes aside when it is floating, which in turn is the weight of a ship (Carlton, 2019).

### 3.7.3 Estimating Force of the Tug

The effective force needed to tug the boat at a given speed in smooth water is known as the resistance.

This is given as $F_T = R_T$, and the power needed to overcome this resistance is the effective power ($P_E$).

$P_E = R_T \times V_S$ (3.14)

But $\eta_D = \frac{P_E}{P_D}$

And $P_D = \frac{P_E}{\eta_D}$ (3.15)

Similarly, $\eta_S = \frac{P_D}{P_S}$ (3.16)

$\eta_D = \frac{1-t}{1-w}\eta_o\eta_R$ (Dabois and Binns, 2018) (3.17)

Where $\eta_R$ is the Relative rotation efficiency which is meant to account for spatial variations in the wake of the vessel which are not captured by the wake fraction as well as induced by the hull. $P_D$, t, w and $\eta_R$ are known.

$P_D$ = Delivered Power (kW), $\eta_S$ = Transmission (shaft line and gearbox) efficiency and $\eta_D$= Delivered efficiency of propeller.

For this case of study, the engines is located towards the stern of the ship, then $\eta_S$= 0.98 or 98% (Hans & Marie, 2013). Again, the engine brake power ($P_B$) is given by,

$\eta_s = \frac{P_S}{P_B}$ (3.18)

Where $\eta_G$ is the efficiency of the gearing system to be used, and for this design a mechanical gearing system will be used hence $\eta_G$=0.93 or 93% (Wilbert, 2019).

### 3.7.4 Design of Propeller

For a twin screw propeller,

i. Wake fraction, w

$= 0.55C_B - 0.20$ (Dabois & Binns, 2018) (3.19)

For the sake of this work, w is large, due to large block coefficient and the distribution of the water velocity around the propeller is very inhomogeneous under such condition. The value of w depends largely on the shape of the hull and also the propeller location and size which has great influence on its efficiency.

**ii.** Thrust deduction fraction t (Dabois and Binns, 2018).

$t = \left(1.67 - 2.3\frac{C_B}{C_{WL}} - 1.5C_B\right) \times w$ (3.20)

But $C_{WL}$ =$C_B + 0.10$ (3.21)

iii. Mass flow rate (Nitonye *et al.,* 2017)

Mass flow $\frac{\text{rate}}{\text{hr}}(\dot{m})$

= total blade area × speed of the ship (3.22)

For Ship speed$V_S$, the Velocity at arriving water $V_A$at the propeller equals speed of advance of the propeller.

Average speed of water through the propeller plane,$V_A$is different, usually less than the speed of the hull$V_S$. The difference between $V_S$ and $V_A$ is called wake velocity $V_W$

$V_w$= $V_S - V_A$ (3.23)

The ratio of the wake velocity $V_w$to the hull speed$V_S$is called wake fraction or Taylor wake fraction w. Mathematically,

$$w = \frac{V_W}{V_S} \quad (3.24)$$

by substitution,

$$w = \frac{V_S - V_A}{V_S}$$

$$w = 1 - \frac{V_A}{V_S}$$

$$\frac{V_A}{V_S} = 1 - w$$

w = 0.15 (wake fraction) depends largely on the hull's shape) (www.wartsilla.com, 12-10-2015)

$V_A$ now becomes

$V_A = V_S(1 - w)$ (3.25)

iv. Hull efficiency of the Tug $\eta_H$

$\eta_H = \frac{P_E}{P_D} = \frac{R_T \times V_S}{T \times V_A} = \frac{1-t}{1-w}$ (Nitonye *et al*., 2017) (3.26)

v. The resultant velocity $V_R$ ((Dabois and Binns, 2018) is expressed as

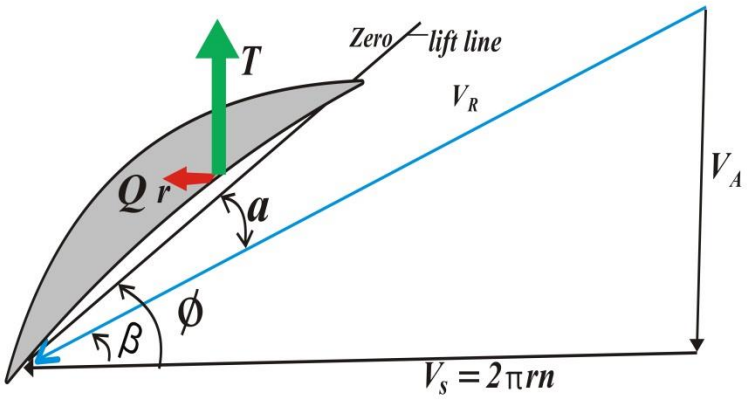


**Figure 3.5:** Velocity and Forces acting on the Propeller

Using Pythagoras theorem to determine the resultant velocity, $V_R$

$V_R^2 = V_A^2 + V_S^2$

But $V_S = 2\pi rn$

$V_R = \sqrt{(V_A^2 + (2\pi rn)^2)}$ (3.27)

The choice in the final design stage may be affected by limitations on propeller diameter and by characteristics of propeller machinery available. The design procedure was restricted to the use of charts and series certified by the Society of Naval Architecture and Marine Engineers [SNAME]. These took into considerations certain propeller chart characteristics like propeller pitch, pitch velocity, pitch ratio, mean axial speed of advance, propeller diameter (D), blade area, number of blades, blade outline, thickness, section shapes which are governed by the need to avoid cavitations, Engine power and rated rpm, effective power ($P_E$) and the ship speed ($V_S$) were fixed. The charts were also

used to explore the best combination of diameter, revolution per minute (rpm) and pitch ratio to give the best efficiency. Ishiodu *et al*., (2013), postulated that once the speed (n) is determined to any corresponding delivered power ($P_D$), it can be estimated on the assumption that moderate changes of loading $\frac{P_D}{n^3}$ would be constant. The material selection procedure shown in Appendix IV also helps to achieve the above.

In design analysis, the open water experiment, diagrams of systematic model propeller series were used. The series consist of propeller whose number of blade (Z), blade area ratio$\left(\frac{A_E}{A_O}\right)$, pitch ratio$\left(\frac{P}{D}\right)$, blade section shape and blade section thickness were varied systematically. The mostly used propeller series is the Wageningen B series. A practical design approach is presented using the Wageningen B series propeller for a case where the$P_D$,$V_A$ and the n are known.

$$B_P = N(P_D) = \frac{P_D^{0.5} N}{V_A^{2.5}} \quad (3.28)$$

Where $B_P$ is the Brake power, delivered power ($P_D$)

The values of $\eta_O$and $\left(\frac{p}{D}\right)$can be traced using charts **(Appendix V)** corresponding to this values of $B_P$.

**(iii) Propeller diameter (D) and the Hub Diameter (d)**

Using the chart of type $B_P$−δ, the values of pitch ratio $\left(\frac{P}{D}\right)$ and optimum diameter($\delta_{opt}$) are obtained as 1.15, and 113m respectively. Hence, calculating the Diameter (D) of the propeller with eqn. 3.29

$D=\frac{\delta_{opt}}{N} V_A$ (Windyandari *et al*., 2018). (3.29)

where $\delta_{opt}$ is the optimum diameter. When propeller diameter (D), is determined the Hub Diameter (d) can be calculated from the Wageningen B-series chart

$d/_D$=0.18 (3.30)

d=0.18D

Also,$\frac{P}{D}$ = 1.15 (3.31)

### 3.7.5 Estimating the Blade area (disc area), Total blade area, Developed area ratio, Expanded area ratio and Projected area ratio

Blade area (Disk area) $A_o = \frac{\pi D^2}{4}$ (3.32)

Total blade area= Blade (disk) area ×disc area ratio (3.33)

Where; Disc (blade) area ratio = 0.51gotten from B-series chart (Prasad & Lanka, 2017). A simple way to avoid cavitation is to increase the blade area ratio and the minimum blade area ratio to avoid cavity was suggested by Keller (Gaafary *et al*., 2010).

Developed area ratio DAR= $\frac{A_D}{A_O} = \frac{4A_D}{\pi D^2}$(3.34)

Expanded area ratio EAR= $\frac{A_E}{A_O} = \frac{4A_E}{\pi D^2}$ (3.35)

$\left|\frac{A_E}{A_O}\right|_{min} = \frac{(1.3+0.3Z)T}{(P_O - P_V)D^2}$+ K (3.36)

The coefficient K equals 0.1 for twin-screws ship (Prasad & Lanka, 2017)

$\left|\frac{A_E}{A_O}\right|_{min}$ =minimum expanded area ratio

EAR and DAR are similar with sections unwrapped from hub largest area ratio hence

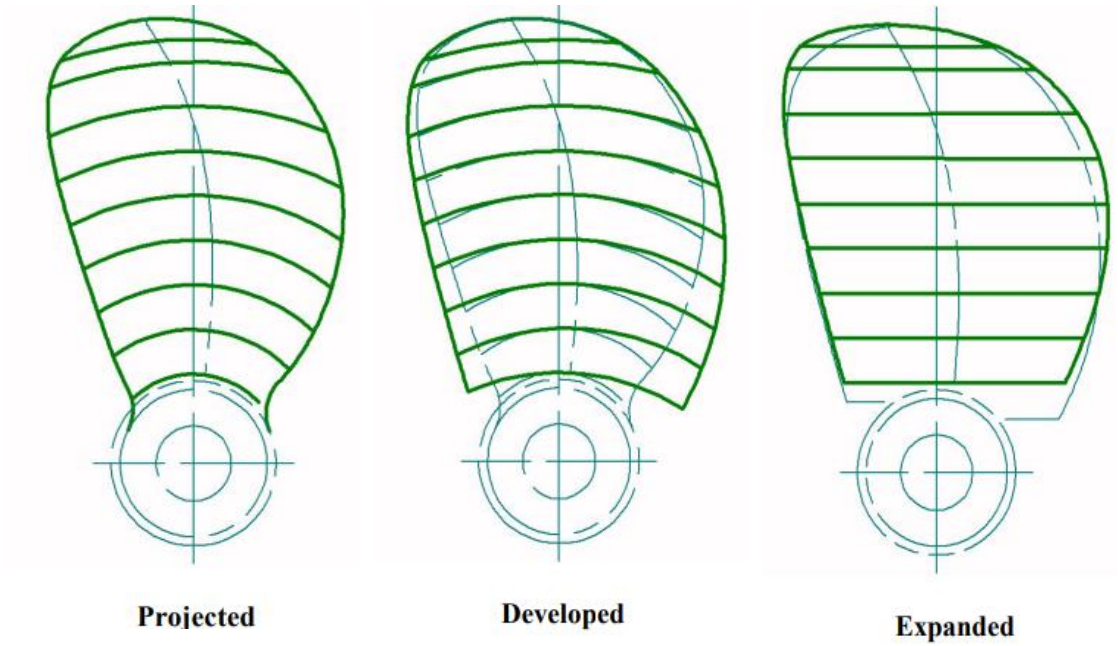


**Figure 3.6:** Projected Area Ratio, Developed Area Ratio and Expanded Area Ratio

$$\frac{A_E}{A_O} = \frac{4A_D}{\pi D^2} \quad (3.37)$$

So, $A_D = \frac{A_E}{A_O} \times \frac{4}{\pi D^2}$

But $\frac{A_E}{A_O} = 0.55$ (from B-series chart)

$\frac{A_D}{A_O} = \frac{A_E}{A_O} = \frac{4}{\pi D^2}$ where $A_D$ (Developed area) and $A_E$ (Expanded area) are equal

Hence $\frac{A_D}{A_O} = \frac{A_E}{A_O} = \frac{4}{\pi D^2}$

$\therefore A_D = A_E = \frac{4A_O}{\pi D^2}$ (Ishiodu *et al*., 2013) (3.38)

However, the projected area of the blade ($A_P$) can be determined using the relationship proposed for non-skewed form as shown below (Ishiodu *et al*., 2013).

$$A_D = \frac{A_P}{1.067 - 0.229\frac{P}{D}}$$

Hence; $A_P = A_D\left(1.067 - 0.229\frac{p}{D}\right)$ (3.39)

Hence the ratio of $A_P$ to $A_D$ can be deduced.

### 3.7.6 Cavitation Criterion (φ)

$$\varphi = 0.7R = P_o - P_v = \frac{1}{2}\rho \times (V \times 0.7R)^2 \quad (3.40)$$

But the relative pressure $(P_o - P_v) = 14.45 + 0.45h$ (3.41)

where φ= Cavitation number, $P_O$=Static Pressure at the shaft centre line, $P_V$ = Vapour Pressure at the shaft centre line ,ρ=water density and 0.7R is the cavitation number calculated based on the static head relative to the shaft centre line and the dynamic head. The thrust loading coefficient $T_C$ is read from Burrill cavitation diagram for uniform flow corresponding to the permissible level back cavitation desired. (See Appendix I)

$$T_c = \frac{\frac{T}{Ap}}{\frac{1}{2}\times l \times V_R^2} = K_T \rho N^2 D^4 \quad (3.42)$$

From equation 3.42,

$$\frac{T}{A_P} = T_c \times \frac{1}{2} \times l \times V_R^2 \quad (3.43)$$

where

N= number of propeller, AP = Projected Area and T = Propeller Thrust.

### 3.7.7 Estimating the Propeller Thrust T and Torque $Q_B$ of the Tug

The propeller thrust T reaction on the main engine is to be applied for designing the main engine shaft system.

**(i) Propeller Thrust (T)**

T= mass flow rate (m) × difference in the velocity (v)

$$T = \dot{m} \times (V_S - V_A) \quad (3.44)$$

But $V_A = V_S \times (1 - w)$

$T = \dot{m}\, V_S\, w$ (3.45)

**(ii) Propeller Thrust Power $P_T$**

$P_T = P_E \times \eta_H = P_E \times \frac{1-t}{1-w}$

$P_T = R_T \times V_A \times \frac{1-t}{1-w}$

But $T = \frac{R_T}{1-t}$

$P_T = T \times V_A = T \times V_S \times (1-w)$ (3.46)

**(iv) Propeller Thrust Force $T_F$**

$\mathbf{T_F} = \frac{P_E}{V_S} \times \frac{1}{1-t}$ (3.47)

But,

$P_E = P_B \times \eta_H \times \eta_O \times \eta_R \times \eta_S$

$P_E = P_B \times \frac{1-t}{1-w} \times \eta_O \times \eta_R \times \eta_S$ (3.48)

**(v) Propeller Engine Thrust $T_E$**

$\mathbf{T_E} = \frac{P_B}{V} \times \frac{\eta_O \times \eta_R \times \eta_S}{1-W}$ (3.49)

Furthermore,

**(vi) Propeller Engine Shaft Torque $Q_B$** $= \frac{P_B}{2\pi \times n}$ (3.50)

Often, $\eta_R$=1.035,$\eta_G$=0.93,$\eta_S$=0.98,$\eta_o$=0.50-0.70,w=0.15 is used (Oleksandr and Valery,2016).

**(vii) The maximum blade thickness**

Blade Thickness Ratio $=\frac{t_o}{D}$ (Ishiodu *et al*., 2013) (3.51)

where $t_o$ is the blade thickness

The blade thickness is at maximum when it is produced to the shaft axis. At maximum,

$t_o=t_{max}$

**(viii) Weight of all blades and the polar moment**

Weight $W = 1.982B_{tf}\varsigma\ YR^3$ (Palle& Lanka, 2017) (3.52)

$I_P=0.2745WR^2$ (3.53)

$I_E = kI_P$ (3.54)

$I_P$=Polar moment of inertia of all blades

$B_{tf}$=Blade thickness fraction (ratio)

$\varsigma$ =blade area fraction (ratio)

Y=Specific weight of blade material

R=Propeller tip radius

Weight W=Mg=Force

The force acting on the propeller F =Mg

**(ix) Stress σ on the propeller**

$$\sigma = \frac{\text{Disk Area of propeller blade}}{\text{Force on the propeller blade}} = \frac{A_O}{F} \quad (3.55)$$

## 3.8 Power requirement analysis

The initial design variable of the propeller as given below (Asina and Ogbonnaya, 2019):

Break power $P_B$=85 hp

RPM = 3000 rpm

Speed $V_S$ = 30.2 knot (in service)

From equation 3.25,

$V_A = V_S(1 - w)$

30.2 (1- 0.15)

25.7 knot

From equation 3.11,

$V_S = 1.34 \times \sqrt{L}$ where *L* is in feet (3.11a)

But $V_S = 1.41 \times \sqrt{L}$ where *L* is in metre (3.11b)

L = Waterline length of the hull ship (Nitonye *et al*.,2017).

For the sake of this study, eqn. 3.11b was used

$V_S = 1.41 \times \sqrt{L}$

$V_S$ = 30.2 Knot =15.54m/s

$\frac{15.54}{1.41} = \sqrt{L}$

$11.02 = \sqrt{L}$

$(11.02)^2 = L$

*L* = 121 m

From eqn. 3.12,

$$F_n = \frac{V_s}{\sqrt{Lg}} = \frac{15.54}{\sqrt{121\ X\ 9.81}} = \frac{15.54}{107.91}$$

$F_n$ = 0.144

From eqn. 3.10,

$R_e = \frac{LV_S}{\gamma}$, $\gamma$ of water is 1.6062 x $10^{-6}$ $m^2/s$

By substitution,

$R_e = \frac{121\ X\ 15.54}{1.6062\ \text{X}\ 10-6} = 1.1707\ \text{x}\ 10^9$

For $R_e$ at $1.1707 \times 10^9$, substituting $R_e$ into eqn.3.9,

$C_F = 0.015011$

$C_R$ is 0.64 (gotten from Gertlers Chart using Froude's number $F_n$ 0.144 and $C_A$ =0.004

Hence, from eqn. 3.5

$C_T = 0.015011 + 0.64 + 0.0004 = 0.6554$

Brake Power ($P_B$) is the power delivered at the engine coupling or flywheel while shaft power ($P_S$) is the output power available at gearbox coupling. The correlation between the Brake Power and Shaft Power (Prasad & Lanka, 2017) is shown in eqn. 3.16 while the formula to calculate the developed power is shown in eqn. 3.18.

$P_S = P_B \eta_S = 85 \times 0.98 = 83.3hp$

where $\eta_S$ is the shaft efficiency and have values of 0.98 for ships with engine located at aft and 0.97 for engine located amid ship(Gaafary *et al*., 2010).For the purpose of this work, 0.98 was used.

The power delivered to the shaft was calculated using eqn. 3.16.

$P_D = P_S \eta_S$

$P_D = 83.3 \times 0.98 = 81.6hp$

Using the chart of type $B_P - \delta$ of Wageningen B-4 series (Ishiodu *et al*., 2013), the Brake Power coefficient ($B_P$) can mathematically be presented as shown in eqn. 3.28,

$$B_P = \frac{P_D^{0.5} N}{V_A^{2.5}}$$

$$= \frac{81^{0.5}}{25.7^{2.5}} N$$

$$= 9 \times \frac{3000}{3348.36}$$

$$= 8.0934 \approx 8.0$$

Using the chart of type $B_P - \delta$, the values of pitch ratio $\left(\frac{p}{D}\right)$ and Optimum diameter $(\delta_{opt})$ are obtained as 1.15, and 113m respectively. Hence, calculating the Diameter (D) of the propeller with eqn. 3.29

$$D = \frac{\delta_{opt}}{N} V_A \qquad (3.29)$$

$$D = \frac{113}{3000} \times 25.7$$

D = 0.97m

Having determined the propeller diameter (D), the Hub Diameter (d) can now be calculated from the Wageningen B series chart

$\frac{d}{D}$ = 0.18 from eqn. 3.30

d = 0.18×0.97

d= 0.174m

But $\frac{p}{D}$ = 1.15 from eqn. 3.31

p = 1.15D = 1.15 × 0.97 = 1.11m

### 3.8.1 Determination of Propeller Thrust T and Torque $Q_B$ of the Tug

From Eqn. 3.44,

Thrust (T) = ṁ ($V_S$–$V_A$)

Where $V_S$ = 30.2knot,$V_A$ = 25.7knot.

From eqn. 3.22,

Mass flow $\frac{\text{rate}}{s}$(ṁ) = total blade area × speed of the boat

Ship speed,$V_S$= 30.2knot = 15.53m/s[1knot = 0.5144m/s]

Total blade area = Total area of the circle × disc area ratio (eqn. 3.33)

Total area of the circle = $\pi r^2$ = 3.142 × $(0.4850)^2$ = 0.7391$m^2$

Given disc area ratio =0.55

Total blade area =0.7391$m^2$ ×0.55 = 0.41$m^2$

Mass flow rate/s (ṁ) = 0.41$m^2$ × 15.53m/s × 1000kg/$m^3$

Mass flow rate/s (m) = 6367.3 kg /s

Eqn. 3.44, now becomes

Thrust (T) = 6367.3 kg /s (15.53m/s - 13.22m/s) = 14.7kN

From Eqn. 3.46,

Thrust Power $P_T = T \times V_S \times (1 - w)$

= 14.7kN × 15.53m/s (1 – 0.15)

= 194.1kW

From Eqn. 3.47,

Thrust Force $T_F = \frac{P_D \eta_O}{V_A}$

$= \frac{81.6 \times 0.56}{25.7}$

= 1.78N/m

From Eqn. 3.49,

Propeller Engine Thrust $T_E = \frac{P_D}{V_A} \times \frac{\eta_O \times \eta_R \times \eta_S}{1-w}$

$= \frac{81.6}{25.7} \times \frac{0.73 \times 1.035 \times 0.98}{1-0.15}$

=2.76 N

Eqn. 3.50 now becomes, Torque $Q_B = \frac{P_B}{2\pi \times n}$

$Q_B = \frac{85}{2\pi \times 3000} = 4.5 \times 10^{-3}$Nm

The blade area (eqn. 3.32) for the type Bp-4 series chart is as follows.

Blade Area $A_O = \frac{\pi D^2}{4} = 3.142 \times (0.97)^2 = 0.739\ m^2$

But Expanded area ratio ($A_E/A$) = 0.55(from B-series chart)

It means $A_E = 0.55A_O = 0.55 \times 0.739\ m^2 = 0.41\ m^2$

where $A_E$ = Expanded area of all blades outside hub

Blade thickness fraction (ratio) = $\frac{t_o}{D}$ (eqn. 3.51)

From $B_p$ – 4 series chart, the maximum blade thickness is when Blade thickness ratio (Blade fraction) = 0.05

$t_0 = 0.05 \times D = 0.05 \times 0.97 = 0.048$m

Hence the maximum blade thickness is 0.048m

### 3.8.2 Developed area ratio, Expanded area ratio and Projected area ratio

In determining the developed and projected areas and their ratios, the following relations were used.

Projected area ratio = $\frac{A_P}{A_O} = \frac{4A_P}{\pi D^2}$

Developed area ratio = $\frac{A_E}{A_O} = \frac{4A_D}{\pi D^2}$

Expanded area ratio = $\frac{A_E}{A_O} = \frac{4A_E}{\pi D^2}$

Recall that D is 0.97m, $\pi$ =3.142

The value of developed area of the blade $A_D$ can be estimated by

$\frac{A_E}{A_O} = \frac{4A_D}{\pi D^2}$

$A_D = \frac{A_E}{A_O} \times \frac{\pi D^2}{4}$

But $\frac{A_E}{A_O}$ = 0.55 (from B-series chart)

$A_D = 0.55 \times 0.739m^2 = 0.41m^2$

Hence $A_D = A_E = 0.41m^2$

It therefore means that the Developed area and the Expanded area of the blade section of the propeller are equal. However, the projected area of the blade ($A_P$) can be determined using the Taylor's approximate formula, relationship proposed for non-skewed form which gives the projected area in terms of the developed area as shown below:

$A_D = \frac{A_P}{1.067 - 0.229\frac{P}{D}}$ (From eqn. 3.39)

Recall:

$\frac{P}{D}$=1.15(from eqn. 3.31- B-series chart)

$A_P = 0.41m^2 \times [1.067 - (0.229 \times 1.15)]$

$A_P = 0.33m^2$

From the foregoing,

Projected area ratio = $\frac{A_P}{A_O} = \frac{0.33m2}{0.739m^2}$ = 0.44

Developed area ratio = $\frac{A_D}{A_O} = \frac{0.41m2}{0.739m^2}$ = 0.55

Expanded area ratio = $\frac{A_E}{A_O} = \frac{0.41m2}{0.739m^2}$ = 0.55

$$\frac{A_P}{A_D} = \frac{0.44}{0.55} = 0.8$$

### 3.8.3 Determination of variation of pitch and thickness along the radius

Suitable distribution of propeller pitch is also an important factor as if there are abrupt canes in pitch, the pressure canes somewhat resembling pulses might affect the blade, causing it to vibrate.

To determine the pitch along the length or radius of the propeller blade at varying percentages, let the varying percentages be 25, 50, 60, 70, 80, 90 and 100 for $p_{0.25}, p_{0.5}, p_{0.6}, p_{0.7}, p_{0.8}, p_{0.9}$ and $p_{1.0}$respectively. Figure 3.7 shows the variation of pitch along the length of the propeller blade.

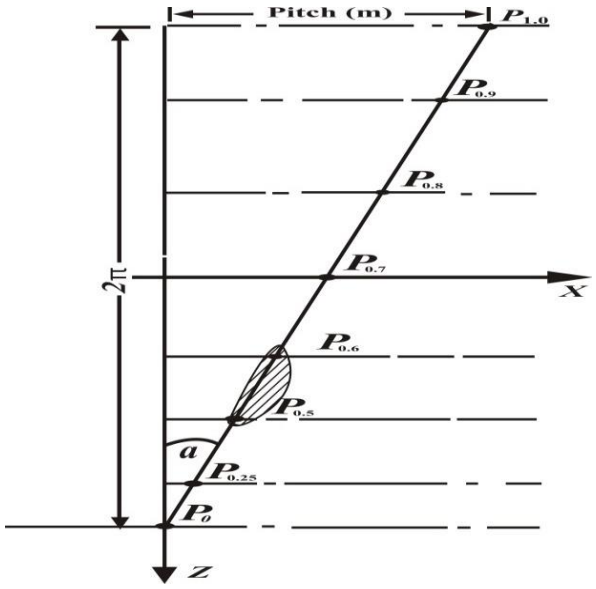


**Figure 3.7:** Variation of pitch along the length of a propeller blade

$R=\frac{D}{2} = \frac{0.97m}{2} = 0.485m$

$p_{itch}$=pitch at i% of R

Pitch $p = p_{ith} \times (R)\left(\frac{p}{D}\right)$

i). $p_{0.25}$ = Pitch at 25% of R

$p_{0.25} = \frac{25}{100} \times 0.485\text{m} \times 1.15 = 0.139\text{m}$

Table 3.4 illustrates the relationship of the pitch radius of the propeller blade at varying percentages.

Similarly, Table 3.5 explains the relationship between the thickness of the blade section along the radius of the propeller and the corresponding percentages which could be found using the blade thickness fraction $\frac{t_o}{D} = 0.05$

Therefore, $t_o$ estimate the thickness along the radius of the propeller

$t_o = 0.05 \times (\text{R Percentage})$

**Table 3.4:** Summary value of Pitch at varying percentage

| $p_{ith}$ | Percentage % | Pitches (m)$\times 10^{-03}$ |
|---|---|---|
| $P_{0.25}$ | 25 | 139 |
| $P_{0.5}$ | 50 | 279 |
| $P_{0.6}$ | 60 | 335 |
| $P_{0.7}$ | 70 | 390 |
| $P_{0.8}$ | 80 | 446 |
| $P_{0.9}$ | 90 | 502 |
| $P_{1.0}$ | 100 | 558 |

$t_{0.1}$ = thickness at 10% of the blades section of expanded cylindrical section

$\therefore t_{ith} = (10\% \text{ of R}) \times 0.05 = 0.1 \times \text{R} \times 0.05$

where R = 0.485m

**Table 3.5:** Summary value of Thickness at varying percentage

| $t_{ith}$ | Percentage % | Thickness (m)× $10^{-03}$ |
|---|---|---|
| $t_{0.1}$ | 10 | 2.42 |
| $t_{0.2}$ | 20 | 4.85 |
| $t_{0.3}$ | 30 | 7.27 |
| $t_{0.4}$ | 40 | 9.70 |
| $t_{0.5}$ | 50 | 12.12 |
| $t_{0.6}$ | 60 | 14.55 |
| $t_{0.7}$ | 70 | 16.97 |
| $t_{0.8}$ | 80 | 19.40 |
| $t_{0.9}$ | 90 | 21.82 |
| $t_{1.0}$ | 100 | 24.25 |

### 3.8.4 Determination of other parameters of designed propeller Blade

Table 3.6 shows values for blade width along its length from the tip of the root spaced at 20 mm interval to each other. The mean width of the propeller blade was determined as follows;

**i. Mean width of propeller blade**

$$\text{Mean width} = \frac{(\text{sum of all the blade width})}{(\text{Number of intervals})}$$

$$\frac{\sum X}{N} = \frac{754.89\times 10^{-3}\text{m}}{8} = 96.9 \times 10^{-3}\text{m}$$

**ii. Width ratio of designed propeller blade**

$$\text{Width ratio} = \frac{\text{Mean developed width}}{\text{Diameter}}$$

$$= \frac{96.9\times 10^{-3}\text{m}}{0.97\text{ m}} = 0.1$$

**Table 3.6:** Values of length from the tip to the root

| S/N | From tip towards the root (m)× $10^{-03}$ | Blade width X (m)× $10^{-03}$ |
|---|---|---|

| | | |
|---|---|---|
| 1 | 20.07 | 50.04 |
| 2 | 39.88 | 80.01 |
| 3 | 59.94 | 95.00 |
| 4 | 80.01 | 109.98 |
| 5 | 100.08 | 124.97 |
| 6 | 119.89 | 134.87 |
| 7 | 139.95 | 109.98 |
| 8 | 160.02 | 50.04 |

Source: Ishiodu *et al*. (2013)

**iii. Length of designed propeller blade**

Determining the length of the blade,

Mean width ratio = $\frac{A_D / \text{Length of blade(outside hub)}}{\text{Diameter D}}$

Mean width ratio × Diameter D = $\frac{A_D}{\text{Length of blade}}$

Length of blade = $\frac{A_D}{\text{Mean width ratio} \times \text{Diameter D}}$

$= \frac{0.41m^2}{0.1 \times 0.97m} = 4.2\text{m}$

The tip radius of the propeller and the radius of the propeller diameter measured from the top of the blade to the center of the propeller boss is approximately the same.

**iv. Weight of all designed propeller blade**

From equation 3.52, the weight of all blades can be calculated.

Weight $W = 1.982 B_{tf} \varsigma Y R^3$

$B_{tf} = 0.05$

$\varsigma = 0.50$

$R = 0.485\text{m}$

Specific weight (W) of substance =

Specific gravity of the material (NAB)× specific weight of water

Where NAB =Nikel Aluminum Bronze

From Appendix A, properties of propeller materials, specific gravity of NAB= 7.6 specific weight of water= 9.807kN/$m^3$

Therefore, specific weight of the propeller blade material is therefore,

Y = specific gravity of NAB × specific weight of water

= 7.6 × 9807 = 74.533kNm-$^3$

Hence, the weight of the blade becomes:

Weight W = 1.982$B_{tf}$ ς $YR^3$

= 1.982×0.05×0.50×74533× $(0.485)^3$

= 420.9N

**v. Polar moment of inertia of designed propeller**

In order to compute the polar moment of inertia of the propeller ($I_P$) and added moment of inertia of the entrapped water ($I_E$), eqn. 3.53 and eqn. 3.54 were used (Mahmud, 2017).

$I_P = 0.275WR^2$ eqn. 3.53

$I_E = KI_P$ eqn. 3.54

where

W = Weight of propeller (N)

R = Radius of the propeller (m)

K is a correction factor and is equal to 0.25

Modulus of Rigidity (G) = 3.861 ×$10^{10}$ N/$m^2$

Hence:

$I_p$=0.275×420.9×0.485$^2$

$I_p$=J$_2$=27.23Nm²

$I_E$=K$I_p$

$I_E$=0.25×27.23Nm²

$I_E$=6.81Nm²

The polar moment of entrapped water ($I_E$) acts as a damper during operation to reduce the effect of vibration. Hence, the effective polar mass moment at the propeller during operation is the contribution of both Torsional moment of inertia of the propeller ($J_2$) and that of the entrapped water ($I_E$).

**vi. Stress on the propeller blade**

Stress = Force per unit area.

Total stress on propeller blade = Force acting per unit area of the blades.

Recall:

Blade (Disk) area $A_0$ = 0.739 m$^2$ from eqn. 3.32

Also, the weight of all blades, W = 420.9N from eqn. 3.52

Since weight is the force acting on the propeller (mass) due to gravity,

F = W = Mg = 420.9 N

Hence, **σ** from equation 3.55 becomes

$$\sigma = \frac{F}{A_O} = \frac{420.9N}{0.739\ m2} = 569.55N/m^2$$

Therefore, the total stress acting on the propeller **σ**= 569.55N/m$^2$

The procedures of propeller design with detailed calculation of the dimensions have been accomplished and the parameters and data are shown in Table 3.8

**Table 3.7**: Summary of calculated results for effective performance

| S/N | PARAMETERS | METRIC UNIT |
|---|---|---|
| 1 | Engine Brake Power ($P_B$ ) | 85 Hp |
| 2 | Ship Speed ($V_S$) | 30.2Knots |
| 3 | Delivered Power of propeller | 80Hp |
| 4 | Propeller speed of advance ($V_A$) | 25.7Knots |
| 5 | Power coefficient ($B_P$) | 8.0 |
| 6 | Propeller open water efficiency ($\eta_o$) | 0.73 |
| 7 | Propeller diameter (D) | 0.97m |
| 8 | Pitch (P) | 1.11m |
| 9 | Pitch ratio (p/D) | 1.15 |
| 10 | Number of blades (Z) | 4 |
| 11 | Blade area ratio ($A_E/A_O$) | 0.55 |
| 12 | Blade thickness fraction ($t_0/D$) | 0.05 |
| 13 | Hub (Boss) diameter ratio (d/D | 0.18 |
| 14 | Blade area (Ao) | 0.739$m^2$ |
| 15 | Expanded area of blade ($A_E$) | 0.41$m^2$ |
| 16 | Developed area blade section ($A_P$) | 0.33$m^2$ |
| 17 | Projected area of blade section ($A_D$) | 0.41$m^2$ |
| 18 | Developed area ratio ($A_D$/Ao) | 0.55 |
| 19 | Expanded area ratio ($A_E$/Ao) | 0.55 |
| 20 | Projected area ration ($A_P$/Ao) | 0.44 |
| 21 | Maximum blade thickness ($t_{max}$) | 0.048m |
| 22 | Boss (Hub) diameter d | 0.174m |
| 23 | Maximum blade width | 134.87 $\times 10^{-3}$m |
| 24 | Mean width ratio | 0.1 |
| 25 | Length of blade | 4.2m |
| 26 | Weight of propeller blades (W) | 420.9N |
| 27 | Polar moment of inertia of propeller blade $I_P$ | 27.23$Nm^2$ |
| 28 | Polar moment of entrapped water $I_E$ | 6.81 $Nm^2$ |
| 29 | Torque $Q_B$ | 4.5 $\times 10^{-3}$Nm |

| | | |
|---|---|---|
| 30 | Thrust T | 14.7kN |
| 31 | Taylor's wake fraction (w) | 0.15 |
| 32 | Force on propeller | 420.9N |
| 33 | Total stress on propeller blades | 569.55N/$m^2$ |

### 3.9 Analysis of Vibration Effect

This part of this study deals with the vibration analysis and methods. This was achieved with the following processes.

#### 3.9.1 Hydrostatic Analyses

Static analysis is performed to calculate pressure by applying a certain load on a physical component either through pointed or equally distributed loads. Here in this case by keeping water medium at a rest position and performing propeller over it hydrostatic load is formed thus it creates stress, strain and deformation over the propeller blade due to concentric pressure created over the propeller. Figure 3.8 shows the boundary condition of tug boat under hydrostatic pressure.

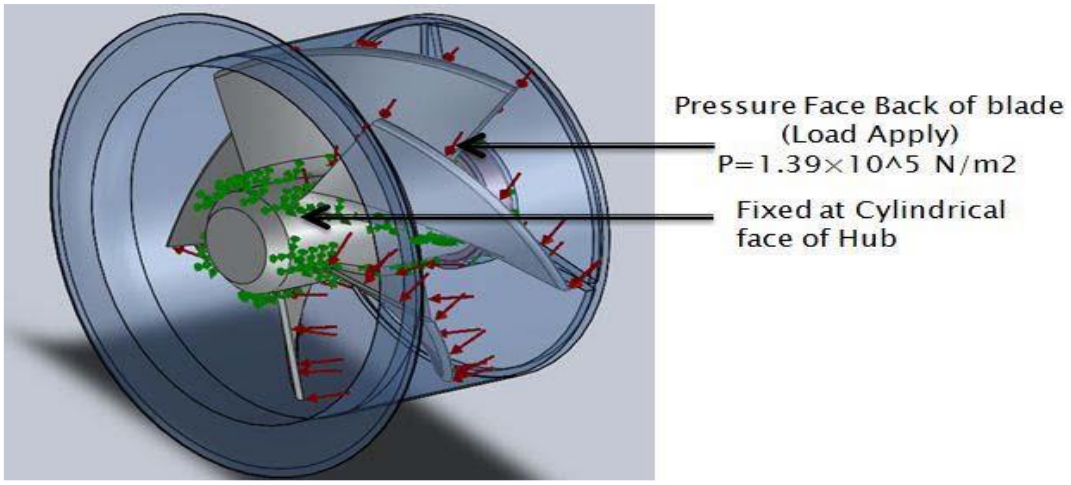


**Figure 3.8:** Boundary layer of tugboat under hydrostatic pressure (Srimanthula *et al*., 2013)

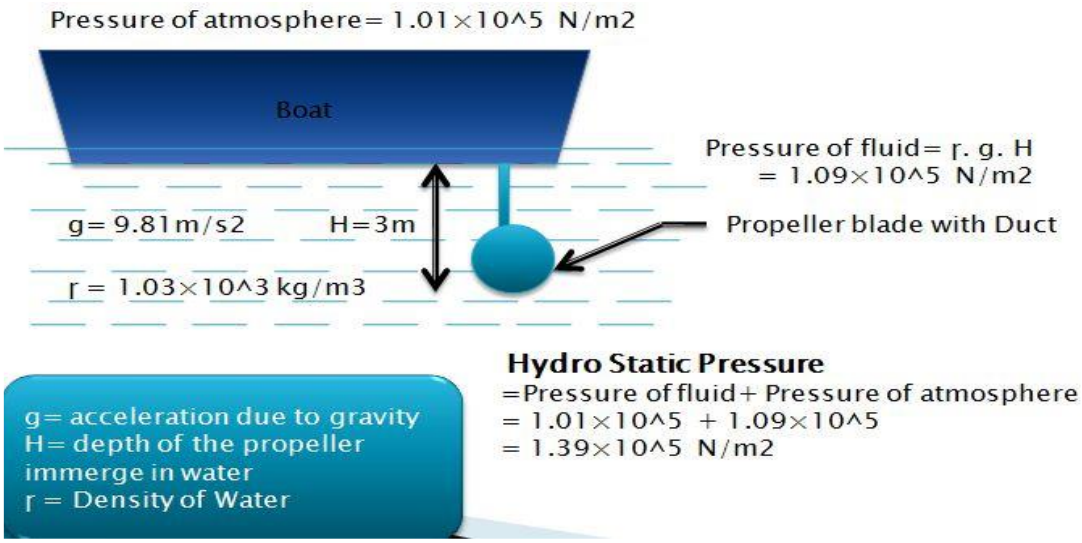


**Figure 3.9:** Hydrostatic pressure on tugboat (Srimanthula *et al*., 2013)

### 3.9.2 Static analysis using Solidworks simulation software

In determining the loads on propulsion system, solidworks advanced computer aided design and simulation software is used. The propulsion system is designed in 3D as seen in Appendix III, for a proper view on the system**.**

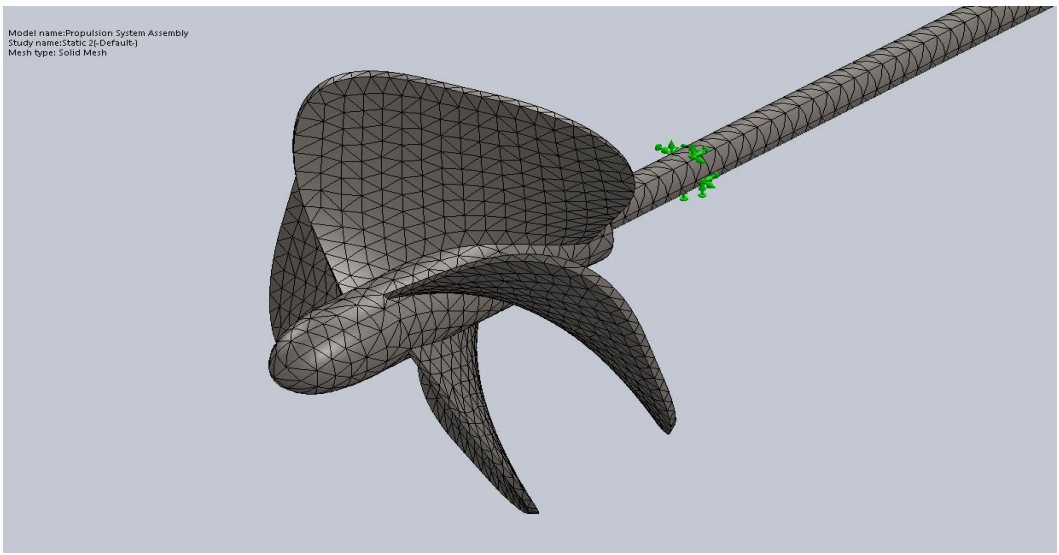


**Figure 3.10:** A 3D Meshed Image of a propeller blade

In achieving this, a project is created and linked with the design of the propulsion system; using the Solidworks static structural model. This helps determine the stress, the deformation of the system upon an impact the strain energy, shear stress and safety factor of the propulsion system. But before it can be achieved, it needs to be discretized (the propulsion system) into smaller elements. This covers all the components and optimizes the shapes of the tetrahedral element amongst the components with smaller curvatures like the spring.

The mesh approach is utilized where a smooth transition of 0.272 was employed for the inflation. The mesh sizes were reduced for curved areas like the spring curves, and this produced a minimum length of 5.8569e-004m. There are a total number of 71926 nodes and 2284 elements.

### 3.9.3 Propeller Blade Static Analysis

Static analysis on 4-blade marine propeller was carried out using solidworks software.

Once the project has been created, stress analysis was carried out and the stress is maximum at the joining points between hub and propeller blades which require using several modeling tools to create the parts and finally assembling the components (see Figure 3.11).

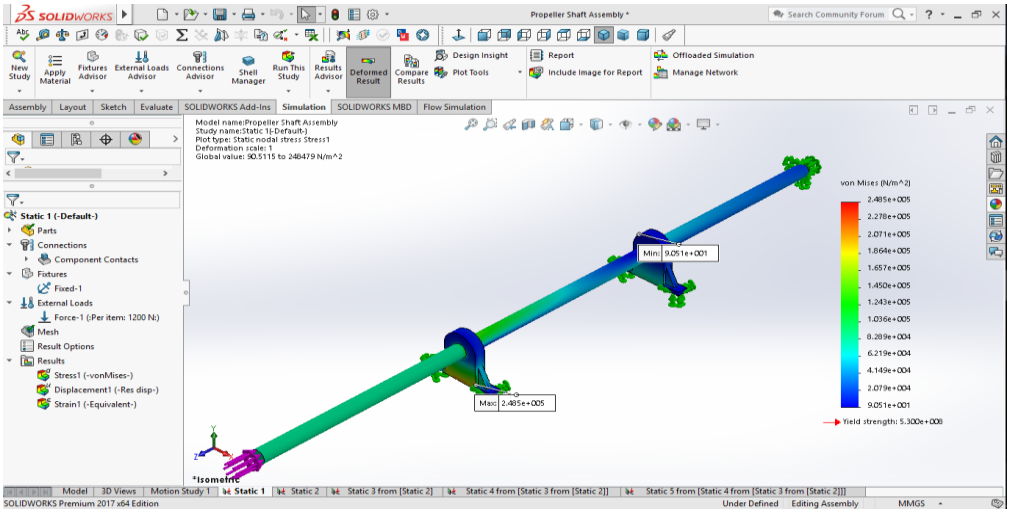


**Figure 3.11:** The project interfaces of solidworks software for a propulsion shaft static analysis

### 3.9.4 Static Structural Results of Propeller blade

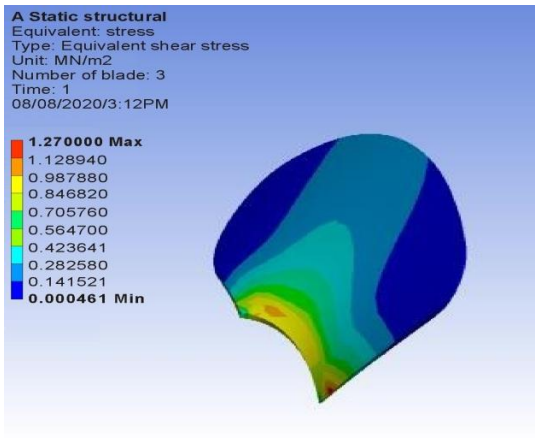


3 – bladed propeller

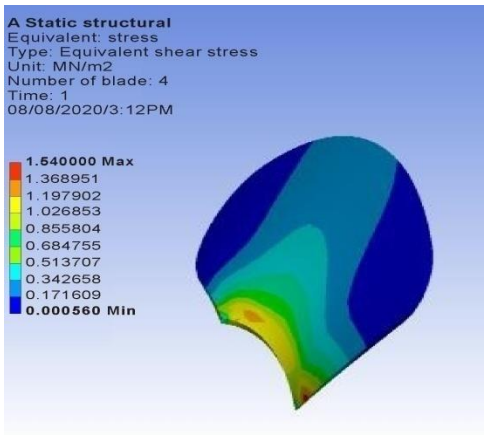


4 – bladed propeller

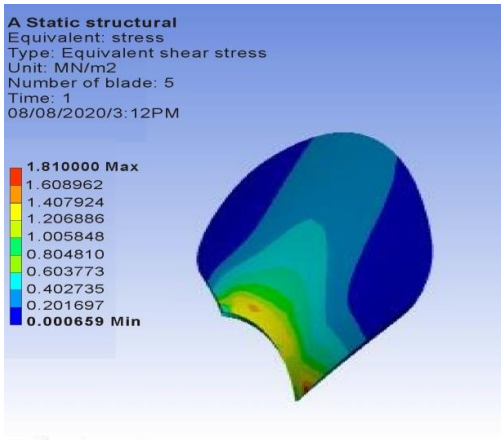


5 – bladed propeller

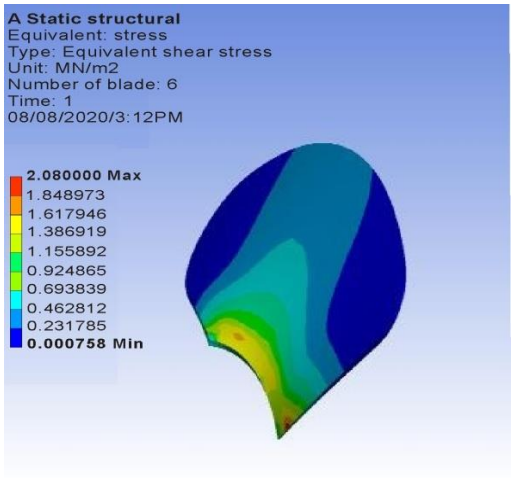


6 – bladed propeller

**Figure 3.12:** Simulation diagram for Static Stress of a Propeller blade at 600rpm

### 3.9.5 Hydrodynamic Analysis

Dynamic analysis is performed when both the medium are in motion during such process a dynamic pressure is created over the physical component calculating the pressure is said to be hydrodynamic pressure. Here in this case the propeller with four different arrangements is analyzed in Solidworks software individually to check the performances of propeller. Figure 3.13 shows the dynamic performance of a propeller.

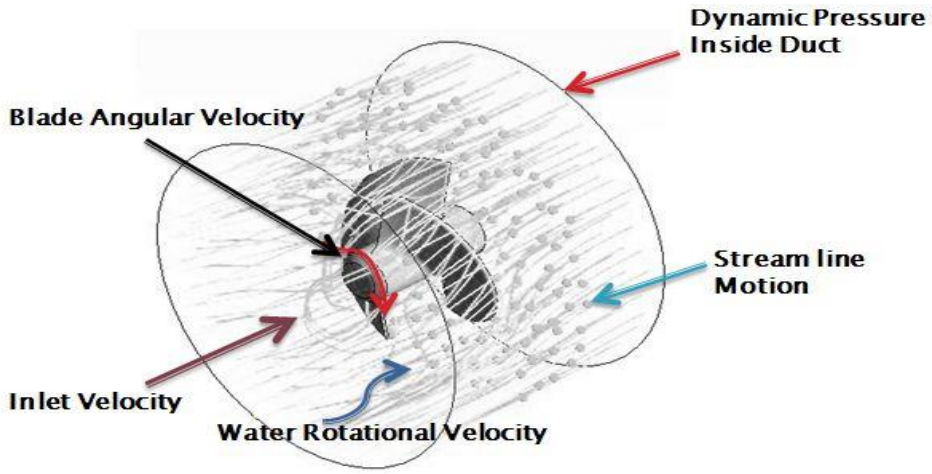


**Figure 3.13:** Dynamic analysis of propeller (Srimanthula *et al*., 2013).

### 3.9.6 Dynamic analysis using Solidworks simulation software

Due to the complexity of the shaft lines which is non-linear, the dynamic modeling and flow simulation (considering the mass effect of water added to the FE model) is performed in solidworks. The geometry of the FE models of shaft lines and the propeller blade for 3, 4, 5 and 6-blade system are designed using the solidworks software by varying the diameters. The dynamics of the engine does not affect the dynamics of the rest of the propulsion system due to the fact that the engine and gear box are connected by using flexible coupling (see Figure 3.14).

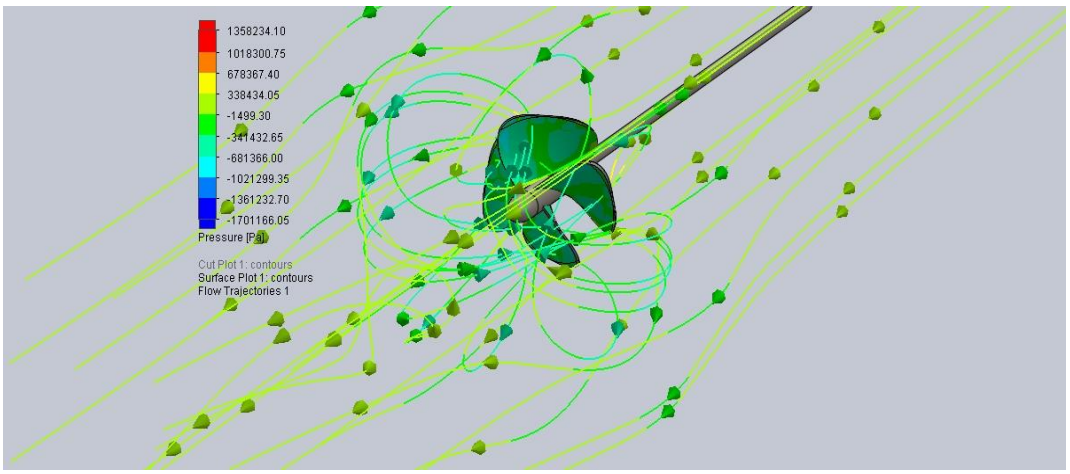


**Figure 3.14:** Model information for dynamic analysis of a propulsion system

### 3.9.7 Process Description

The following is the description of the processes carried out during simulation.

- Analysis Type was External-exclude cavities without flow condition and internal space.
- The rotation and reference axis were selected as rotating axis (i.e Z-axis).
- The fluid selected was water and flow type was laminar and turbulent.
- Wall thermal conditions was taken as adiabatic and roughness as 0 micrometer (consider smooth surface of propeller).
- The pressure used was 101.325kPa and temperature as 293.2k.
- Velocity of flow entered at inlet was 7.08m/s in direction of rotating axis.

The value of outlet axial velocity and thrust force developed (force) for various rotating speed in rad/s was then determined.

For a fixed RPM (600RPM) the propulsion system is subjected to a variable mass flow simulation and the pressure induced on the blade surface were noted and recorded. The number of the propeller blade was varied from 3-blade to 6-blade and was subjected for a mass flow with the aid of the simulation tool. And the minimum and maximum pressures built-up are noted and recorded. Figure 3.15 below is a typical example of the flow simulation for a 4-blade system.

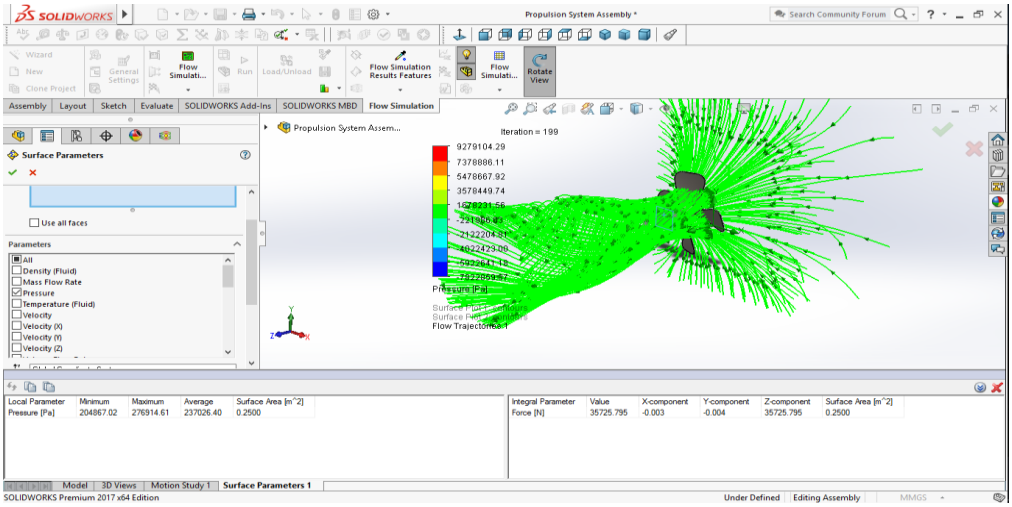


**Figure 3.15:** Simulation diagram of a propulsion system for a 4-blade propeller

The thrust force obtained for 600rpm rotation of propeller is 14.7kN with outlet axial velocity of 25.7Kn (13.221m/s). The mass of this propeller was 29.38kg and total blade area o was 0.739m$^2$.

### 3.9.8 Effect of increasing RPM on Propeller blade performance.

Higher RPM equate to more fuel burnt in the same amount of time and more power produced. Running at lower RPM equates to higher torque and thus lower horsepower but increases efficiency. High RPM get much worse nearing max RPM. Max RPM is that limit that the engine can take before severe damage. Running at near max RPM for extended periods will drastically reduce engine life. Each force produced was used to determine the hydrodynamic pressure for different number of blade at varying RPM (see Figure 3.16 and Figure 3.17).

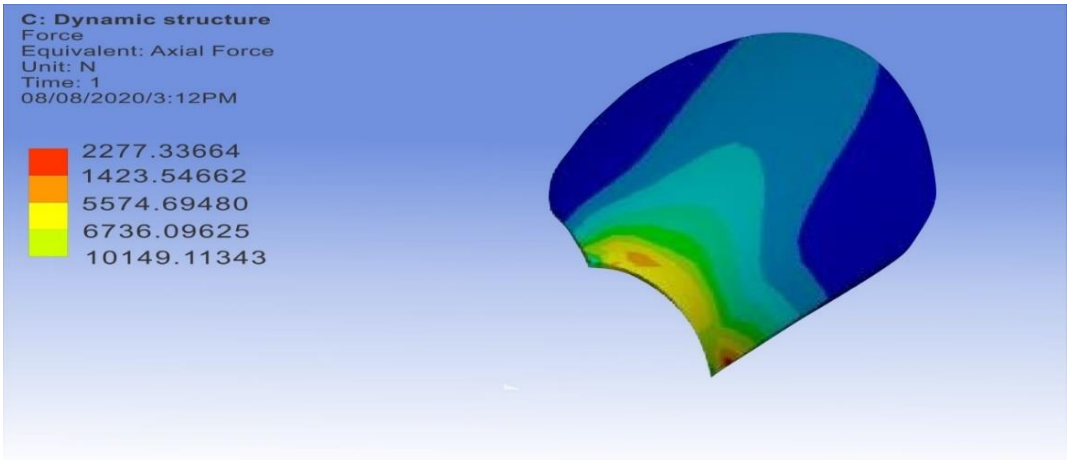


**Figure 3.16:** The simulation of dynamic analysis of forces produced for propeller blade at varying RPM

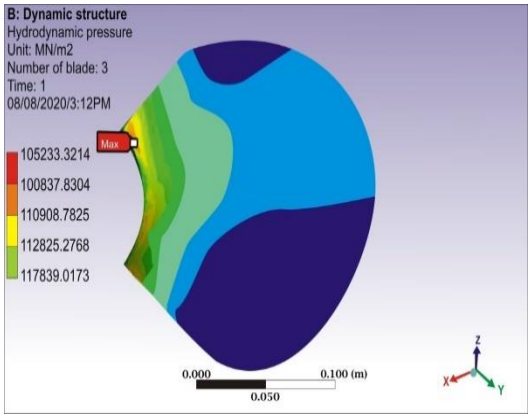


3 blade propeller

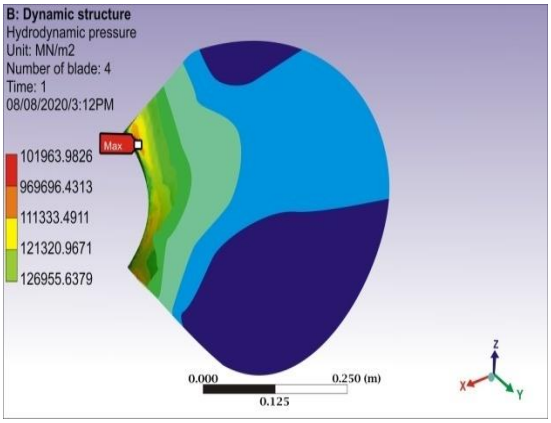


4 blade propeller

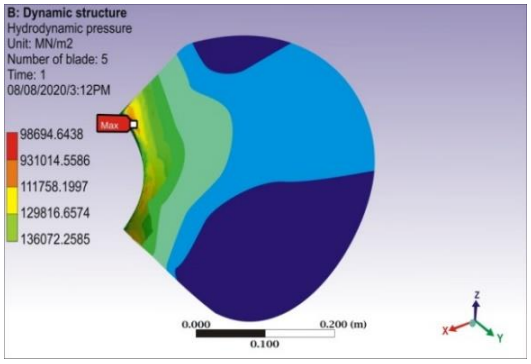


5 blade propeller

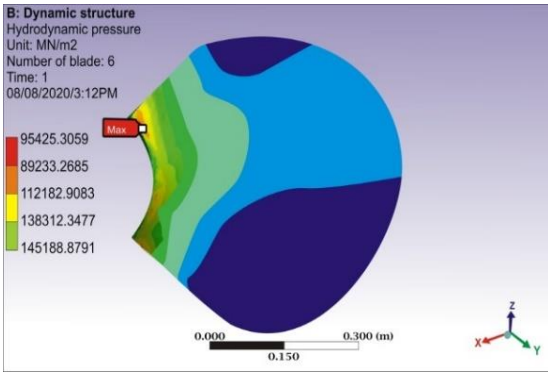


6 blade propeller

**Figure 3.17:** The simulation of dynamic analysis of hydrodynamic pressure for propeller blade at varying RPM

### 3.9.9 Effect of velocity distribution along the propeller blade

The propeller forces produced due to an angular velocity of pitch are analyzed and are shown to be very small for the pitching velocities that may actually be realized in maneuvers with the exception of the spin. The rotational flow produced by the propeller depends on the number of blades (n=3, 4 and 5 in this study). Velocity distribution at different parts of the solution domain was also studied. Figure 3.18 and Figure 3.19 shows simulation of the velocity distribution carried out and the forces produced along the propeller blade at rake angle $4.05^0$.

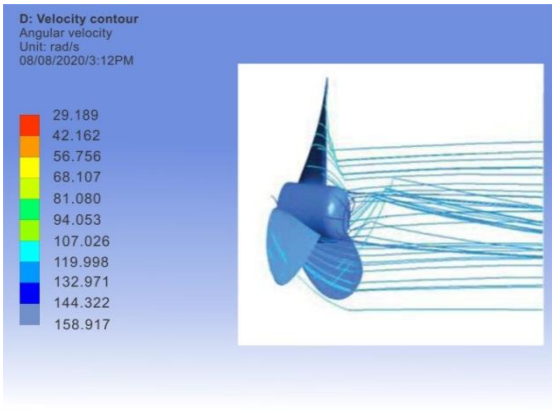


3- bladed propeller

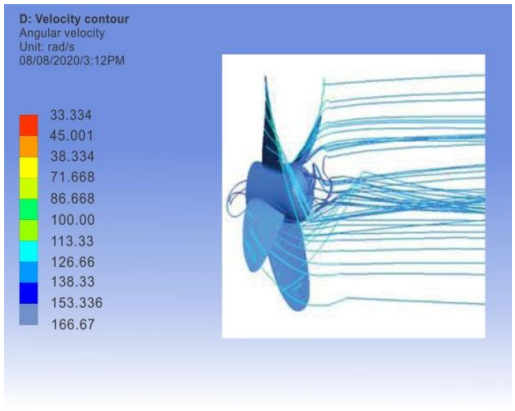


4-bladed propeller

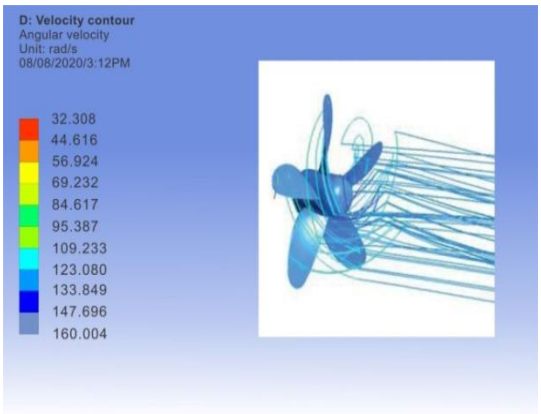


5-bladed propeller

**Figure 3.18:** Velocity distribution along the propeller blade at rake angle $4.05^0$

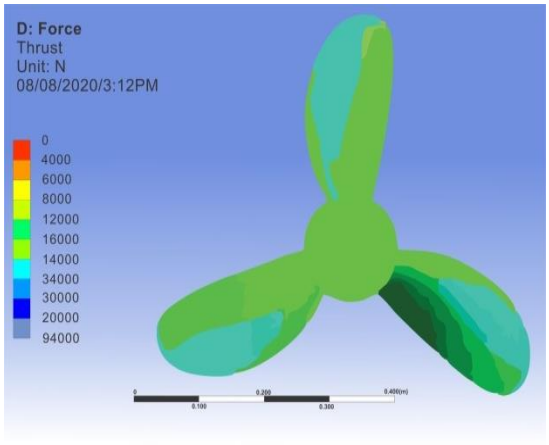


3-bladed propeller

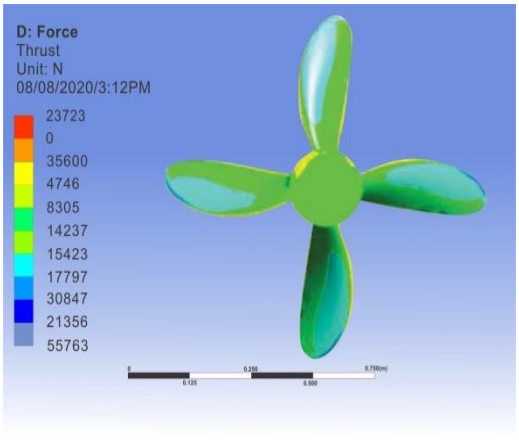


4-bladed propeller

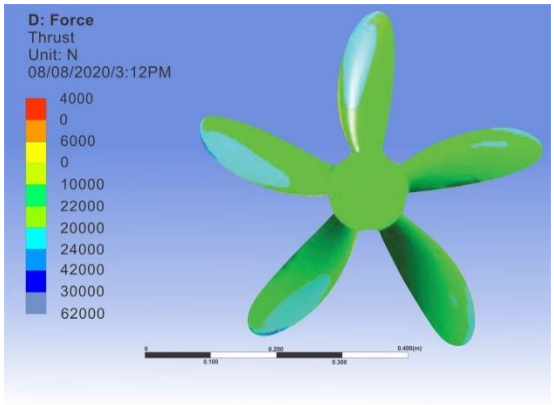


5-bladed propeller

**Figure 3.19:** Thrust (Force Produced) along the propeller blade at rake angle $4.05^0$

# CHAPTER FOUR

# RESULTS AND DISCUSSIONS

## 4.1 Results

The result deduced from the problems formulation and solution method, as prescribed in the previous chapter is interpreted here in this chapter. You may recall that the concept design phase is the phase in which possible failures can be avoided or mitigated. A suitable value of the 2nd order vertical moment at which excitation is not likely to occur considering the power of the propeller engine is used.

### 4.1.1 Results on 2nd order vertical moment prediction

In Table 4.1 is an excel spread sheet showing the results/output values of $M_{2V}$ at varied PRU is presented. The output value of 2nd order vertical moment (N-m) is gotten from the manufacturer. Let the values of P and PRU be arbitrarily selected to be PRU=100kW, 120kW and 220kW and P be 1500kW, 1600kW, 1700kW, 1800kW and 2000kW (see Figure 3.1).

**Table 4.1:** Result/output values of $M_{2V}$ at varied PRU value

| **PRU** | **Result($M_{2v}$)** | | | | |
|---|---|---|---|---|---|
| 100 | 150000 | 160000 | 170000 | 180000 | 200000 |
| 120 | 180000 | 192000 | 204000 | 216000 | 240000 |
| 220 | 330000 | 352000 | 374000 | 397000 | 440000 |

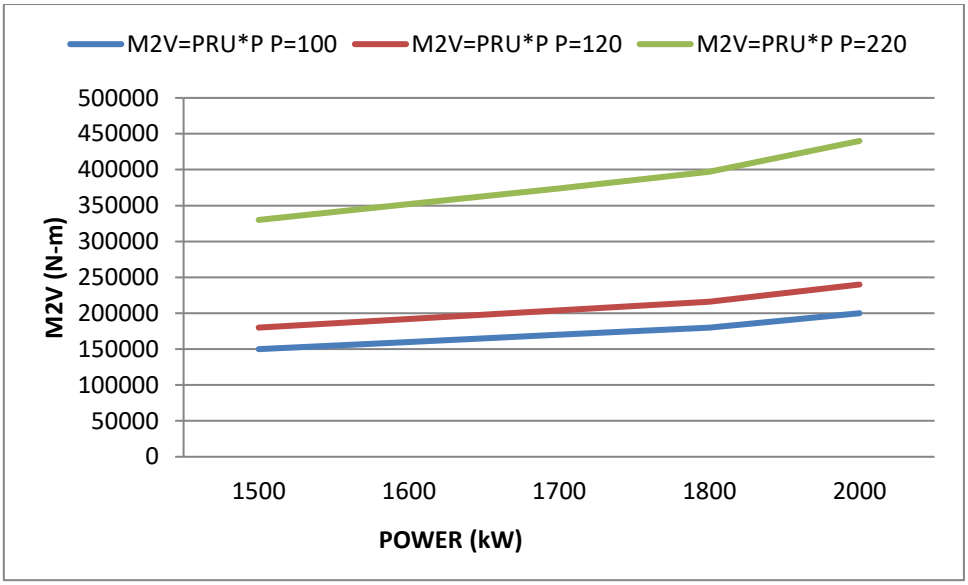


**Figure 4.1:** Graphical representation of the value of the 2nd order vertical moment (N-m) at different engine power, and power related unbalance scale value.

Table 4.1 above serves as a guide to a prospective customer to purchase propeller's engine, as it gives the designer to decide the course of action to be followed showing the maximum and minimum $2^{nd}$ order vertical moment value at 250000kW/N-m and 5000kW/N-m respectively against the maximum and minimum engine power of 2000kW and 1500kW respectively on the ground that engine with this rating limit is cleared for excitation. Thus, in practice, during the design phase the designer should ensure the required value of $M_{2V}$ is gotten from the potential main engine manufacturer, as early as possible, since $M_{2V}$ is the most concern of diesel engine excitation.

### 4.1.2 Mitigation of Excitation Problem / Stiffness Determination

Table 4.2 shows the results for stiffness using the stiffness optimization model in equation 3.2 for k*i* at varied values of m and ω, given that the mass ($4.53 \times 10^6$kg) of the tugboat.

**Table 4.2:** Output parameters and values

| Concept | Symbol | Model | Output |
|---|---|---|---|
| Deflection | y | $y = \frac{FD^3}{d^4G}N$ | 189831.63 |
| Spring constant | k | $k = \frac{F}{y}$ | 298.15896 |
| Critical damping ratio | Cc | $Cc = 2\sqrt{(kM)}$ | 82160.324 |

Table 4.3 below shows the stiffness value of a propulsion system which is designed with the aim to maneuver a tug of 5000 tons and also shows that the stiffness of a propulsion system, diameter and thickness of the propeller shaft are proportionately related as the increase in the former result to increase in the later. These values of shaft diameter are constants and can be affected by allowable deflection and the stiffness (see Appendix II).

**Table 4.3:** Value of stiffness and deflection on varying the value of the diameter and thickness of the propeller shaft

| S/No | Shaft Diameter (m) | Thickness (m) | Deflection y (m) | stiffness k |
|---|---|---|---|---|
| 1 | 10.5 | 16.0 | 189831 | 298.15896 |
| 2 | 11 | 17 | 171262.77 | 330.4863 |
| 3 | 11.5 | 18 | 155698.38 | 363.52337 |
| 4 | 12 | 19 | 142498.38 | 397.19749 |
| 5 | 12.5 | 20 | 131186.96 | 431.44533 |

### 4.1.3 Propeller performance improvement

The parametric analysis is carried out on propeller blade using solidworks simulation software, by varying the number of propeller blades, the relative velocity of the water and the propellers rotation per minutes(RPM) at a given propeller blade radius of 0.485m (see Figure 4.2)

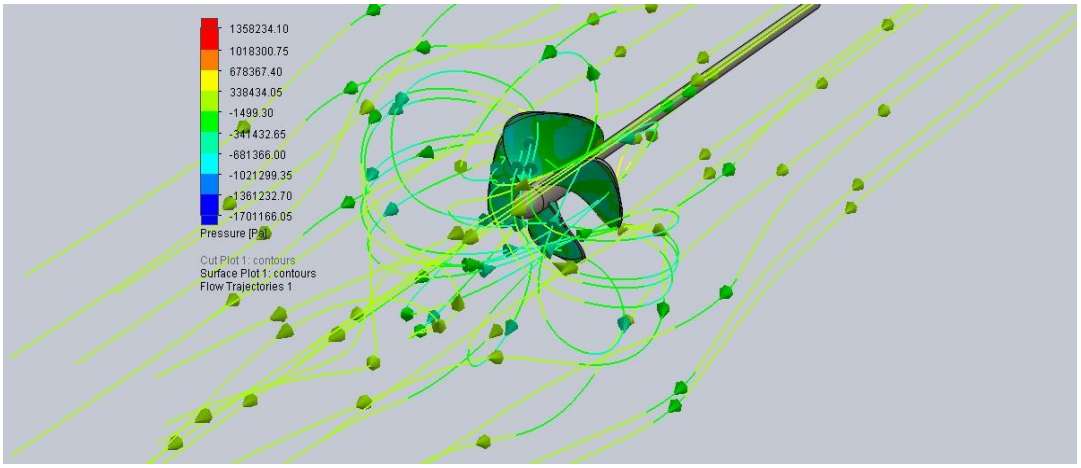


**Figure 4.2:** The performance of the blade on dynamic simulation

In this project, static and dynamic analysis is performed on ducted propeller blade with 3-blade, 4-blade, 5-blade and 6-blade arrangements. Performance of each propeller blade was checked by applying hydrostatic and hydrodynamic loading. During the loading condition 3-blade ducted propeller performed at 1.27MN/m$^2$ maximum shear stress performed at hydrostatic loading, while that of 4-blade, 5-blade and 6-bladeducted propeller performed at 1.54MN/m$^2$, 1.81MN/m$^2$ and 2.08MN/m$^2$ respectively at constant RPM (600RPM). For the hydrodynamic condition, all the ducted blades performed at 0.249MN/m$^2$ maximum shear stress at 475RPM, 486.1RPM, 461.2RPM and 454.3RPMrespectively (see Table 4.4).

**Table 4.4:** Results of propeller blade from static and flow analysis using solidworks simulation software.

| ***MAXIMUM SHEAR STRESS(N/m^2)*** | ***MINIMUM SHEAR STRESS(N/m^2)*** | ***ANGULAR VELOCITY (rad/s)*** | ***APP.ROTATION PER MINUTES(RPM)*** | ***NUMBER OF BLADES N(-)*** |
|---|---|---|---|---|
| *MAXSS(N/m^2)* | *MINSS(N/m^2)* | *RRP rad/s* | *App.RPM* | *Nos. of Blades* |
| *2.49E+05* | *9.05E+01* | *49.7783* | *475* | *3* |
| *MAXSS(N/m^2)* | *MINSS(N/m^2)* | *Engine rad/s* | *App.RPM* | *Nos. of Blades* |
| *1.27E+06* | *4.61E+02* | *62.831* | *600* | *3* |
| *MAXSS(N/m^2)* | *MINSS(N/m^2)* | *RRP rad/s* | *App.RPM* | *Nos. of Blades* |
| *2.49E+05* | *9.05E+01* | *49.018* | *468.1* | *4* |
| *MAXSS(N/m^2)* | *MINSS(N/m^2)* | *Engine rad/s* | *App.RPM* | *Nos. of Blades* |
| *1.56E+06* | *5.60E+02* | *62.831* | *600* | *4* |
| *MAXSS(N/m^2)* | *MINSS(N/m^2)* | *RRP rad/s* | *App.RPM* | *Nos. of Blades* |
| *2.49E+05* | *9.05E+01* | *48.258* | *461.2* | *5* |
| *MAXSS(N/m^2)* | *MINSS(N/m^2)* | *Engine rad/s* | *App.RPM* | *Nos. of Blades* |
| *1.85E+06* | *6.59E+02* | *62.831* | *600* | *5* |
| *MAXSS(N/m^2)* | *MINSS(N/m^2)* | *RRP rad/s* | *App.RPM* | *Nos. of Blades* |
| *2.49E+05* | *9.05E+01* | *47.497* | *454.3* | *6* |
| *MAXSS(N/m^2)* | *MINSS(N/m^2)* | *Engine rad/s* | *App.RPM* | *Nos. of Blades* |
| *2.43E+06* | *7.58E+02* | *62.831* | *600* | *6* |

The data shown in Table 4.4 also explains that increase in the number of propeller blade also increases the propeller performance which is the increased RPM for dynamic analysis while that of static analysis remains constant for the propeller required to overcome a vessel.

The data also shows that increase in the number of propeller blade leads to a corresponding increase in the shear stress values.

### 4.1.4 Result of effect of velocity distribution along the propeller blade

Tables 4.5, 4.6 and 4.7 show that the number of blade and the frequency of the propeller increases simultaneously ($N \alpha f$) for three to six bladed propeller. The force produced

increases which leads to the possible excitation as a ratio of the natural frequency to the deduce frequency approaches unity. By increasing the number of blade, angular velocity is decreased. This is graphically represented in Figures 4.3, 4.4 and 4.5 respectively. The possibility of reducing vibration problem is by increasing the number of propeller blades. Hence, the position of Yuriy (2006) on DNV recommendations for propeller excitation amplitude is justified.

**Table 4.5:** Angular velocity at rotating region using a propeller of three blade design at increasing PRM

| Force produced (N) | 0 | 4000 | 6000 | 8000 | 12000 | 16000 | 14000 | 34000 | 30000 | 20000 | 94000 |
|---|---|---|---|---|---|---|---|---|---|---|---|
| α [rad/s] | 29.189 | 42.162 | 56.756 | 68.107 | 81.080 | 94.053 | 107.026 | 119.998 | 132.971 | 144.322 | 158.917 |

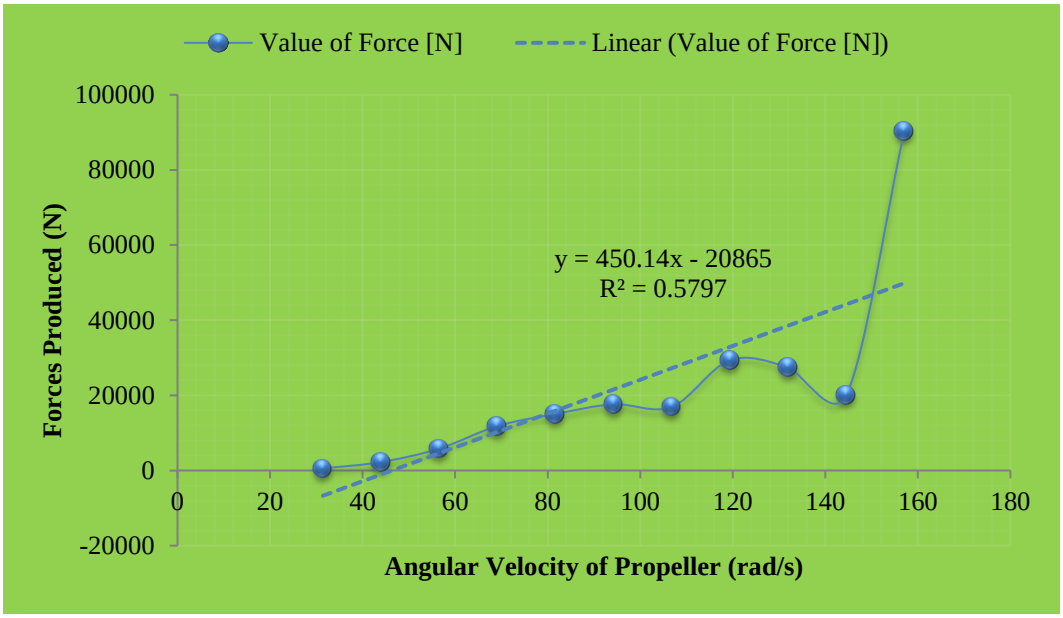


**Figure 4.3:** Propeller parametric study for three blade design showing the value of forces

**Table 4.6:** Angular velocity at rotating region using a propeller of four blade design at increasing RPM

| | | | | | | | | | | | |
|---|---|---|---|---|---|---|---|---|---|---|---|
| Force produced (N) | 23723 | 0 | 3560 | 4746 | 8305 | 14237 | 15424 | 17797 | 30847 | 21356 | 55763 |
| α [rad/s] | 33.334 | 45.001 | 58.334 | 71.668 | 86.668 | 100.002 | 113.335 | 126.669 | 138.336 | 153.336 | 166.670 |

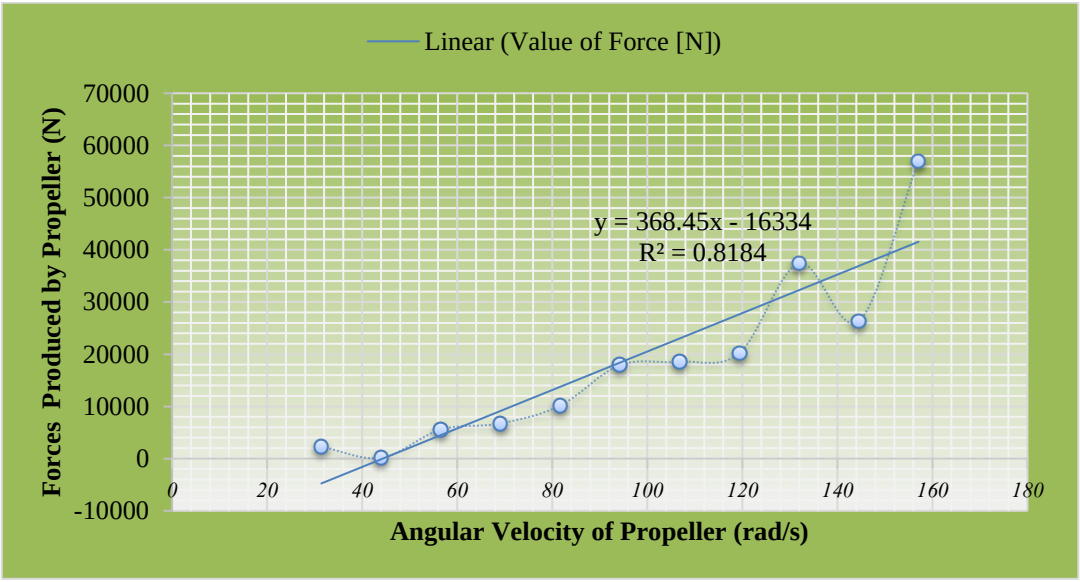


**Figure 4.4:** Propeller parametric study for four blade design showing the value of forces.

**Table 4.7:** Angular velocity at rotating region using a propeller of five blade design at increasing RPM

| | | | | | | | | | | | |
|---|---|---|---|---|---|---|---|---|---|---|---|
| Force produced (N) | 4000 | 0 | 6000 | 0 | 10000 | 22000 | 20000 | 24000 | 42000 | 30000 | 62000 |
| α [rad/s] | 32.308 | 44.616 | 56.924 | 69.232 | 84.617 | 95.387 | 109.233 | 123.080 | 133.849 | 147.696 | 160.004 |

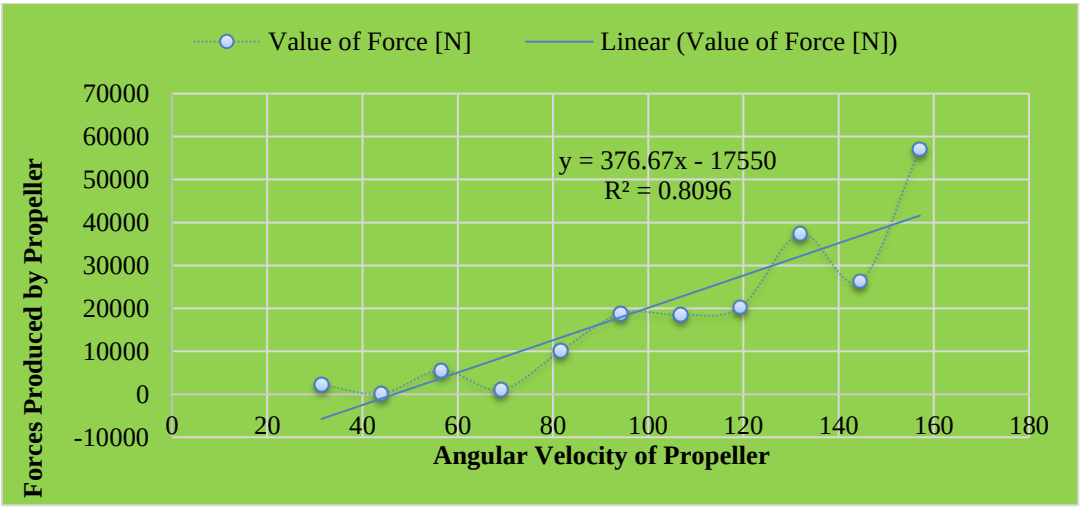


**Figure 4.5:** Propeller parametric study for five blade design showing the value of forces.

### 4.2: Vibration Analysis

In this analysis, the strength and vibrational characteristics of the propeller blade are evaluated which can be static analysis or dynamic analysis as discussed below.

#### 4.2.1: Static Analysis

The static analysis of the various propeller blades with the aid of Solidworks static structural model helps in the determine the distribution of maximum and minimum stresses as shown in the Table 4.8

**Table 4.8:** Result of the static load on the propulsion system (extract from Table 4.6)

| Propeller type | Ratings | Stress($Nm^{-2}$) |
|---|---|---|
| 6 Blades | Maximum | 2.08 E+06 |
| | Minimum | 7.58 E+02 |
| 5 Blades | Maximum | 1.81 E+06 |
| | Minimum | 6.59 E+02 |
| 4 Blades | Maximum | 1.54 E+06 |
| | Minimum | 5.60 E+02 |

| | | |
|---|---|---|
| 3 Blades | Maximum | 1.27 E+06 |
| | Minimum | 4.61 E+02 |

Material Yield Strength = 2.78 E+07

Table 4.8 explains the effect of increase of number of blades on the propeller as shown in Figure 4.6 below. For a design of tugboat of 600RPM having a mass of 4.53 x $10^6$kg with 3 propeller blade can maneuver without causing any possible damage on the propulsion system having a maximum stress of 127MN/$m^2$ on the shaft is less than the material yield stress of 278MN/$m^2$.On increasing the number of blades from 3 to 4, 5 and 6. Maximum shear stress also increased to 154MN/$m^2$, 181MN/$m^2$ and 208M N/$m^2$ respectively which could lead to possible failure of the propeller blade and the entire propulsion system if more blades are added.

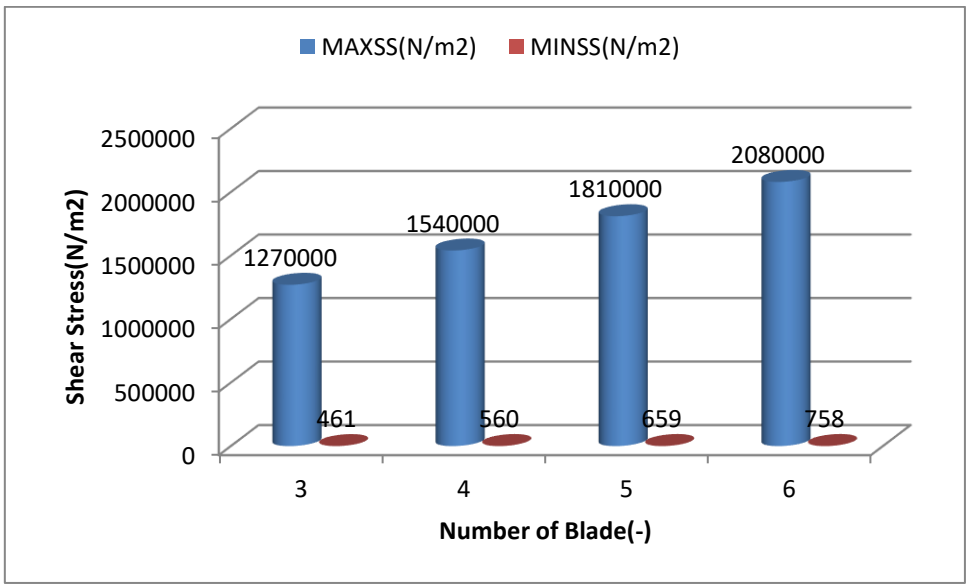


**Figure 4.6:** Maximum and Minimum Shear Stress value at variable blade number at 600RPM.

### 4.2.2 Dynamic Analysis

The dynamic analysis of the various propeller blades with the aid of Solidworks dynamic structural model helps in determining the hydrodynamic average pressure of propeller

blades due to the force (Thrust) at varying RPM presented in Table 4.8 (see Figure 3.16 and Figure 3.17).

**Table 4.9:** Result of Surface Propeller parameter under varied mass of water

| Value of force (N) | Average Pressure(Pa) for 3 blade | Average Pressure(Pa) for 4 blade | Average Pressure(Pa) for 5 blade | Average Pressure(Pa) for 6 blade |
|---|---|---|---|---|
| 2277.33664 | 105233.3214 | 101963.9826 | 98694.6438 | 95425.3059 |
| 142.354662 | 108837.8304 | 96969.64313 | 93101.45586 | 89233.2685 |
| 5574.694804 | 110908.7825 | 111333.4911 | 111758.1997 | 112182.9083 |
| 6736.096248 | 112825.2768 | 121320.9671 | 129816.6574 | 138312.3477 |
| 10149.11343 | 117839.0173 | 126955.6379 | 136072.2585 | 145188.8791 |

The surface propeller parameter for flow trajectory shows that at increasing the number of blade, the mass of water impelled also increase; thereby increasing the pressure build up on the surface of the blade, and the result is the possible failure of the propeller over time. This is represented graphically in Figure 4.7

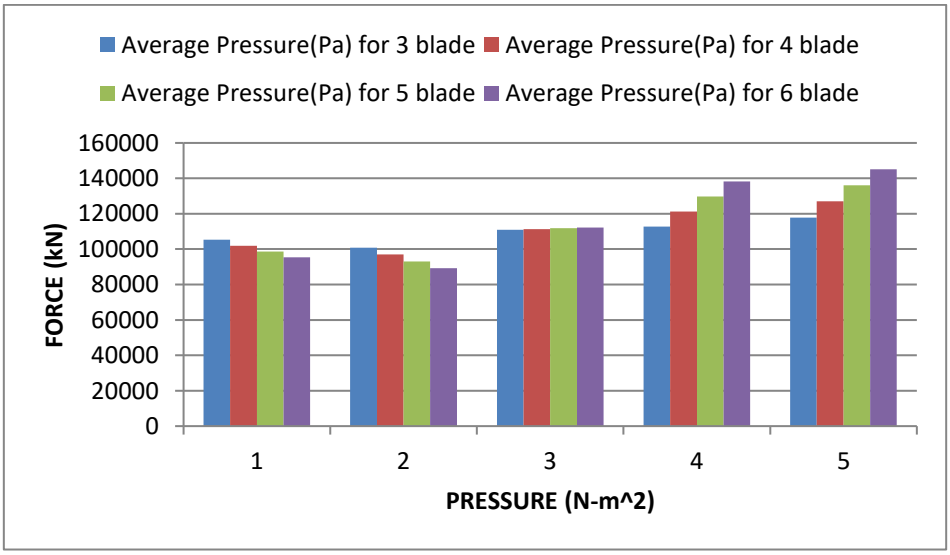


**Figure 4.7:** Average pressure build-up on the blade as a result of variable blade number.

The two graphs in Figures 4.8 and Figure 4.9 below originates from Table 3.5 and Table 3.6 respectively were seen to increase linearly, which means that the pitch and thickness of the blade increased linearly from the blade hub intersection up to the tip of the blade.

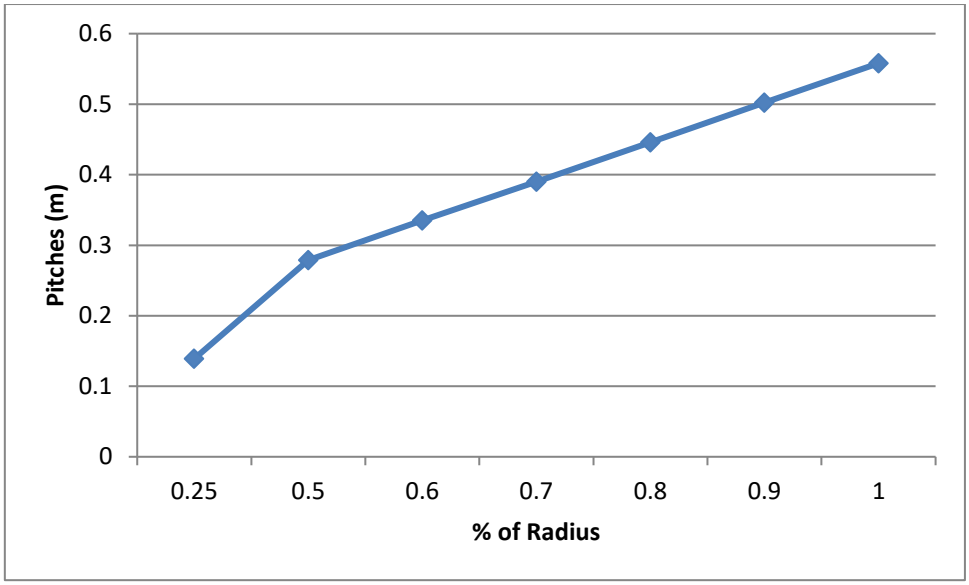


**Figure 4.8:** Values of Pitches at varying Percentages

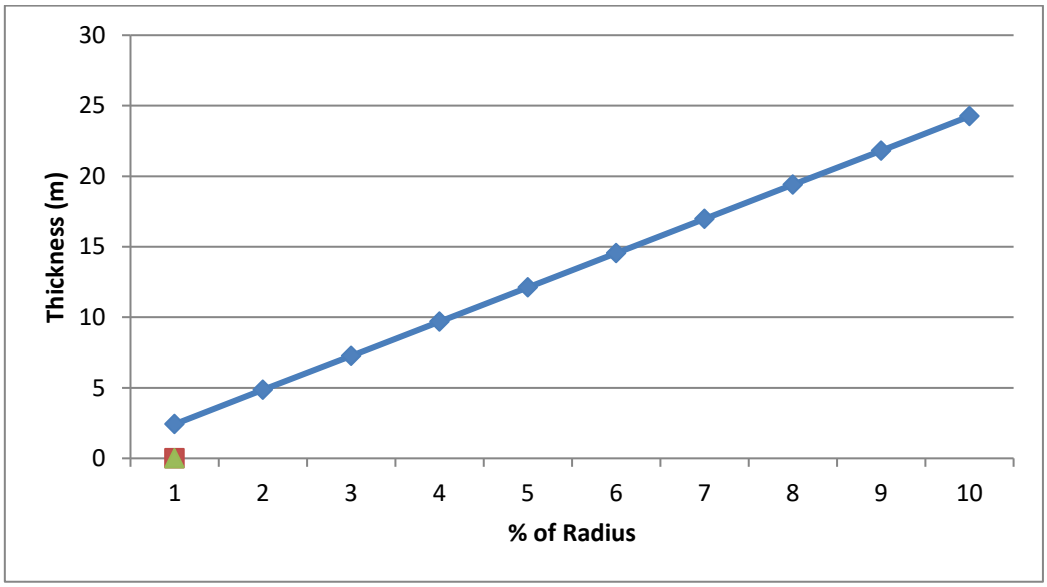


**Figure 4.9:** Values of Thickness at varying Percentages

# CHAPTER FIVE

# CONCLUSION AND RECOMMENDATIONS

## 5.1 Conclusion

The following deductions were made

- Some Properties (diameter, cord length, pitch, torque and efficiency) of the propeller were determined to ascertain the amount of power that a propeller can absorb and deliver thus dictating the amount available for propulsion.
- The design analysis of effective power carried out was used as a basis for selecting the main engine and designing of a suitable propeller capable of propelling the tugboat for the various sea states. Effective power is estimated and the tug resistance is overcome.
- Four types of propeller blade (3, 4, 5 and 6-bladed) were simulated and the simulation result shows that on increasing the number of propeller blades the efficiency drops due to higher thrust with more drag which reduces fuel efficiencies and result from interfering propeller streams.
- On increasing the number of propeller blades the vibration is reduced and the performance of the propulsion system is increased. High level of cabin vibration can cause stress and sailors fatigue and may lead to hearing problems for the crew members.
- Varying propellers of tugboat to be used in tropical sea state like Nigeria was provided with the view to ascertain maximum and minimum allowable pressure in the propulsion system.

## 5.2 Recommendations

The researcher therefore gives the following recommendation:

- Before considering an activity in a mechanical structure, a static and dynamic loading analysis should be conducted on a propulsion system.

- For high RPM propellers in operation, there should be caution and moderations as there may be no need to increase the number of propeller blades.
- The variation of the numbers of the blade design in a propeller should not be based only on performance optimization, but its tendency to fail considering the RPM of the engine and the radius of the propeller blades.
- For further studies a computational fluid dynamic simulation (CFD) analysis using other software like ANSYS to compare results and a response surface analysis could help in achieving more detailed results through the use of more advanced tool and statistical tools.
- The $B_p$ Charts Series 4.55 should be adopted for the designs of 4-bladed propellers which are Charts developed from tested basin experiments.

### 5.3 Contribution to Knowledge

The models analyzed from this study will be very useful in the Marine and Logistics Industries when selecting propulsion for improves performance.

This result of the study will serve as a reference to the Maritime Companies on the concept design phase of a tug boat considering the number of the propeller blade on the ground that the RPM of the machine compensate for the performance of the propeller, thus there may be no need to increase the number of blade as it could result to the issue of negative pressure built-up and in turn could lead to the failure of the propulsion system.

When selecting cutting variables to save production time, cost and energy for performance improvement, reduced emission and decrease total production costs of machined parts.

## REFERENCES

Adil, E. B. & Fulgence, R. (2014). Fluid-Structure Interaction Effects on the Propulsion of a Flexible Composite Monofin: *Journal of Engineering Volume 2014(2014), Article ID 541953,8 pages*

Ajay, B. P. & Tejas S. P. (2019). Design and simulation of Marine propeller with different blade geometry. *International journal of innovative science and resources. Volume 20 pp 128*

Altosole1, M. & Figari, M. (2011). Effective Simple Methods for Numerical Modelling of Marine Engines in Ship Propulsion Control Systems Design

American Bureau of shipping (2006): Guidance notes on ship vibration (updated January 2015 and then 2018).

Amirhossein, A., Mahdi, M. &Mehran, N. (2015). Multidisciplinary Design Optimization and Analysis of Hydrazine Monopropellant Propulsion System: *International journal of Aerospace Engineering Volume 2015, Article ID 295636, 9 pages.*

Arjun, B. C., Ejaaz, A. V., Rao, M. & Akash (2018). Static and Dynamic Analysis of a ship Propeller – IJSER. *International Journal of science and engineering research vol9, issue 3.*

Asina, M. & Alfred, E. O. (2019). Vibration Analysis of a 3 bladed Marine propeller shaft for 35000DWT bulk carrier EJERS. *European Journal of Engineering Research and service vol4 no, 10.*

Aulia, W., Gunawan, D. H. & Suharto. S. (2018). Design and performance analysis of B-Series propeller for traditional purse seine boat in the north coastal region of the central java Indonesia.

Blade area ratio defined – A hydrocomp Technical reports report 15.

*International journal of Aerospace Engineering Volume 2015, Article ID 295636, 7 pages.*

Bose, N., Insel, M., Anzbock, R. & Toki, N. (1999). Final Report and Recommendations to the 22nd ITTC from the Specialist Committee on Unconventional Propulsors. *Proceedings from the* 22$^{nd}$ *ITTC.*

Carlton, J. S. (2019) Marine propeller and propulsion (5$^{th}$ edition) *European Journal of Engineering Research and service vol4 no, 16 pp 204*

Dabois, A. & Binns, J.R. (2018). Estimation of a ship's nominal wake fraction through full scale speed trials. *European Journal of Engineering Research and service vol4 no, 15 pp 305.*

Diagram: page 13 same as 21: fixed pitch Marine propeller geometry Design issue 11 page no 1131-1138

Emilia, S. & Jarosław, P. (2015). Methods of calculating ship resistance on limited waterways: *Polish Maritime Research Vol. 21; Pp. 12-17*

Fauzi, W., Dini O., Dominicus, D., Syamsul, H & Bambary P. (2019).The effect of blade thickness and number of blade to cross flow wind turbine performance

using 2D CFD simulation. *International journal of innovative Technology and Exploring engineering (IJITEE) Vol. 26; Pp. 62*

Franklin, J. D. R. (2013). Review of cases of propulsion systems in which noise, vibration, or fracture problems have existed. *Ship Science & Technology-Vol.7-n.13-(65-74) July 2013-Cartagena (Colombia)*

Franklin, J. D. R. (2013). Analysis of most frequent cases of vibration in propulsion system *Journal of Marine Engineering & Technology -Vol.7 Pp 19*

Gaafary, M. M., El-Kilani H. S., Moustafa M. M. (2010). Optimum design of B-Series Marine Propellers. . *International journal of innovative Technology and Exploring engineering (IJITEE) Vol. 15; Pp. 32*

Geertsma, D. R., Negenborn , R. R.,Visser, K. & Hopman, J. H.(2017). Design and control of hybrid power and propulsion systems for smart ships: A review of developments: *Applied Energy Journal homepage: www.elsevier.com/ locate/apenergy. Vol. 25; Pp. 50*

Hai,L., Shuli, W., Ying H., David C.Y.& Zhang, Y. L. (2015).Optimal sizing of hybrid PV/diesel/battery in ship power system. *Journal homepage: www.elsevier.com/ locate/apenergy Vol. 34; Pp.120*

Hans, O. K., Marie, L. (2013). Prediction of resistance and propulsion power of ships. Pp 150

Hasan, J. & Hamid, A. (2015). Model identification and dynamic analysis of ship propulsion shaft lines. *Journal of Theoretical and Applied Vibration and Acoustics1(2)85-95(2015)*

Herman,V. A. (2001). Structural Dynamics Modeling using Modal Analysis. S*LmsInternational Inter-Leuvenlaan 68, B-3001 Leuven , Belgium Vol. 5; Pp. 49*

Ishiodu, A., Williams, E., Ezenwa, O. & Kuvie, E. (2013). Design procedure of 4 bladed propellers
*International journal of innovative Technology and Exploring engineering (IJITEE) Vol. 30; Pp. 24*

Jesse, A., Allan, B. & Yue, Q. (2012). EN 40 Dynamics and vibrations
*International journal of innovative Technology and Exploring engineering (IJITEE) Vol. 217; Pp. 24*

Jose, J. A. & Hameed, J. H. (2015). Design and Analysis of Propeller Shaft: *International Journal of Innovative Research in Science, Engineering and Technology, Vol. 4*

Katarzyna, Z. (2014). A simplified method for calculating propeller thrust decrease for a ship sailing on a given shipping lane: *Polish Maritime Research 2(82) 2014 Vol 21; Pp. 27-33*

Kiam, B. Y., Rosalam S., Wen Y. H. & Cheah, M. O. (2014). Effects of marine propeller performance and parameters using CFD method. *Journal of applied science vol14, issue 22, page no 3083-3088.*

Krishnankutty, P. (2015). Ship Resistance and Propulsion. Indian Institute of Technology, Madras. Pp 123

Kumar, G. S., Hayatul, I. M. & Rakibul, H. (2019). Marine propeller modeling and performance analysis using CFD tools. *AIP Conference Proceedings 2121,040012*

Lindgren H., Aucher M., Gross A. and Tamura K. (1978). Report of Performance Committee. 15*th ITTC Proceedings*, 15*th International Towing Tank Conference in the Hauge*, The Netherlands.

Mahiou,F., Fulgence, R.,Bideau, N. & Rakotomanana L. R. (2015).Influence of the Fluid-Structure Interaction on the Modal Analysis, and on the Dynamics of Composite Monofin: Optimization of Propulsion: Arts et Métiers Paris Tech,2 Bd du Ronceray,49035 Angers, France.

Mahmud, K.(2017). Ship design project and presentation. http:teacher.buet.ac.bd/mmkarim/propellerlecture.pdf
*Makili Enterprise Vol.23 Pp 10.*

Martinez, I. (1995). Marine Propulsion -Selecting an Efficient Propulsion System. *Isidoro Martinez Enterprise.Pp 304*

Minsk, M. P. (2013). Diesel Engines Operation Manuals. *Minsk Motor Company, Plant Holding. Volume 2013, Article ID 8145646,7 pages.*

Nengqi, X., Ruiping, Z., Xiang, X. & Xichen, L. (2016). Vibration of Marine Diesel-Electric Hybrid Propulsion System: *Hindawi Publishing Corporation Mathematical Problems in Engineering Volume 2016, Article ID 8130246,9 pages.*

Nitonye, S., Adumene, S. & Howells, U. U. (2017). Numerical design and performance analysis of a tugboat propulsion system. *International Journal of Engineering and Technology*, (*IJET*) *Germany*, **4**, 500-946

Nturamato, F., Masu, L. & John, B. kirabira (2018). Novel application of Aluminium Metal Matrix composites. Pp 39

Nitonye, S. & Adumene, S. (2015). Comparative Modeling of Hull Form Resistance for Three Ocean Going Vessels Using Methodical Series. *International Journal of Engineering and Technology*, (*IJET*) *Germany*, **4**, 489-496.http://www.sciencepubco/index.php/IJET.comhttps://doi.org/10.14419/ijet.v4i4.4948

Nitonye, S. (2017). Design Calculation for Equipment and Components Specification of Lubricating Oil System of a Tug Boat: *International Journal of Advances in Engineering & Technology, Vol. 10, Issue 3*

Ole, G., Carne, G. T.& Lauffer P. J. (1998). The Natural Excitation Technique (Next) for modal parameter extraction from operating structures. *International Journal of Analytical and Experimental Modal Analysis, Vol.10,No 4,pp.260-277,1998.*

Oleksandr ,B. & Valery, N. (2016). Effectiveness Harbour Tugboat: Problem Formulation and Methodology of its Solution.

Palle, P. & Lanka, B. B. (2017). Design and Analysis of the propeller blade. *International journal of Advance in Mechanized and Civil Engineering, ISSN: 2394-2827 vol-4, issue 2*

Prasad, P. & Lanka B. B. (2017): Design and analysis of a propeller blade. *International journal of Advance in Mechanized and Civil Engineering, ISSN: 2394-2827 vol-4, issue 2*

Qianwen, H., Jia, L., Cong, Z. & Yan, X. P. (2012). Analysis on propulsion shafting coupled torsional-longitudinal vibration under different applied loads. *Journal of Sound and Vibration.2003;261:359-364.*

Ravikant, G. K., & Mukesh, D. W. (2013). Modal Analysis of drive shaft using FEA: *International Journal of Engineering and Measurement Research, Vol.-3,Issue-1,ISSN No.:2250-0758 pages:4-7*

Saqlain ,A., & He L. (2007). Optimization and Sizing for Propulsion System of Liquid Rocket Using Genetic Algorithm: *Chinese Journal of Aeronautics 20*.

Seetharama, Y. R., Millikarjuma, K. R. & Sridttar, B. R. (2012). Stress Analysis of composite Propeller by using Finite Element Analysis. *International Journal of Engineering Science and Technology (IJEST)*

Sen,I. S. & Minoru, K. (2015). Torsional Vibration Characteristics of Marine Diesel Propulsion System Installed with Highly-Elastic Rubber Coupling, *Report presented at Iranian society of acoustics and vibration. 2003;641:359-674.*

Serdar, B. (2014). Ship theory-propulsion: Propeller Design and Cavitation

*International Journal of Emerging Technology and Advanced Engineering, Volume 4, issue 18*

Srimanthula, S., Bodapalli, J. & Gudimetla, A. (2013). Design, Static and Modal Analysis of A Propeller Shaft for Reducing Vibrations Using Composite Damping: *International Journal of Emerging Technology and Advanced Engineering, Volume 3, issue 10.*

Sofras, E. & Prousalidis, J. (2014). Developing a new methodology for evaluating diesel—electric propulsion; *Journal of Marine Engineering & Technology, 13:3, 63-92ISSN: 2046-4177 (Print) 2056-8487 (Online)*

Soria, L., Peeters, B., Anthonis, J. & Herman, V. A. (2012). Operational Modal Analysis and the performance assessment of vehicle suspension systems: *IOS press and the authors, Belgium.*

Takaaki,N. & Hiroyasu, K. (2016). A study on fuel saving effect in hybrid propulsion system for tug boat: *Proceeding of 7th PAAMES and AMEC. International Journal of Emerging Technology and Advanced Engineering, Volume 4, issue 18*

Vidya ,M. S , Venkaiah, M. & Sumil, D. (2013). Static and Dynamic Analysis of Composite Propeller of Ship Using FEA: *International Journal of Engineering Research & Technology (IJERT), ISSN: 2278-0181, Vol. 2*

Vince, D. H., Harford, K., Stapleton, R. and Robert, A. (2016). Resolving the tugboat energy equation: *International Journal of Emerging Technology and Advanced Engineering, Volume 4, issue 18*

WARTSILA Encyclopedia of the marine technology www.wartsilla.com (12-10-2015)

Wilbert, W. (2017). Basic Principles of ship propulsion https://www.researchgate.net>publication>320329671

Windyandari, A. , Dwi, H. & Suharto, S.(2018).Design and performance analysis of B-Series propeller for traditional purse seine boat in the North coastal region of central Java Indonesia

Wu, X. (2010). A Rapid Development Process for Marine Propellers through Design, Simulation and Prototyping.

www.marineinsight.com (2019): Types of vibrations in ships – Hull girder vibration.

www.usna.edu>courses(2012). Prediction of Ship Resistance and Propulsion Power (Project no. 2010-56).

www.engineeringtoolbox.com, 20/09/2020

Yuriy, B. (2006). Torsional Vibration Calculation Issues with Propulsion System using Shaft Designer Shaft Calculating Software: *Publishers, NL-2984 CB Ridder kerk, The Netherland. Volume 2006*

**APPENDIX I**

Burrill cavitation diagram

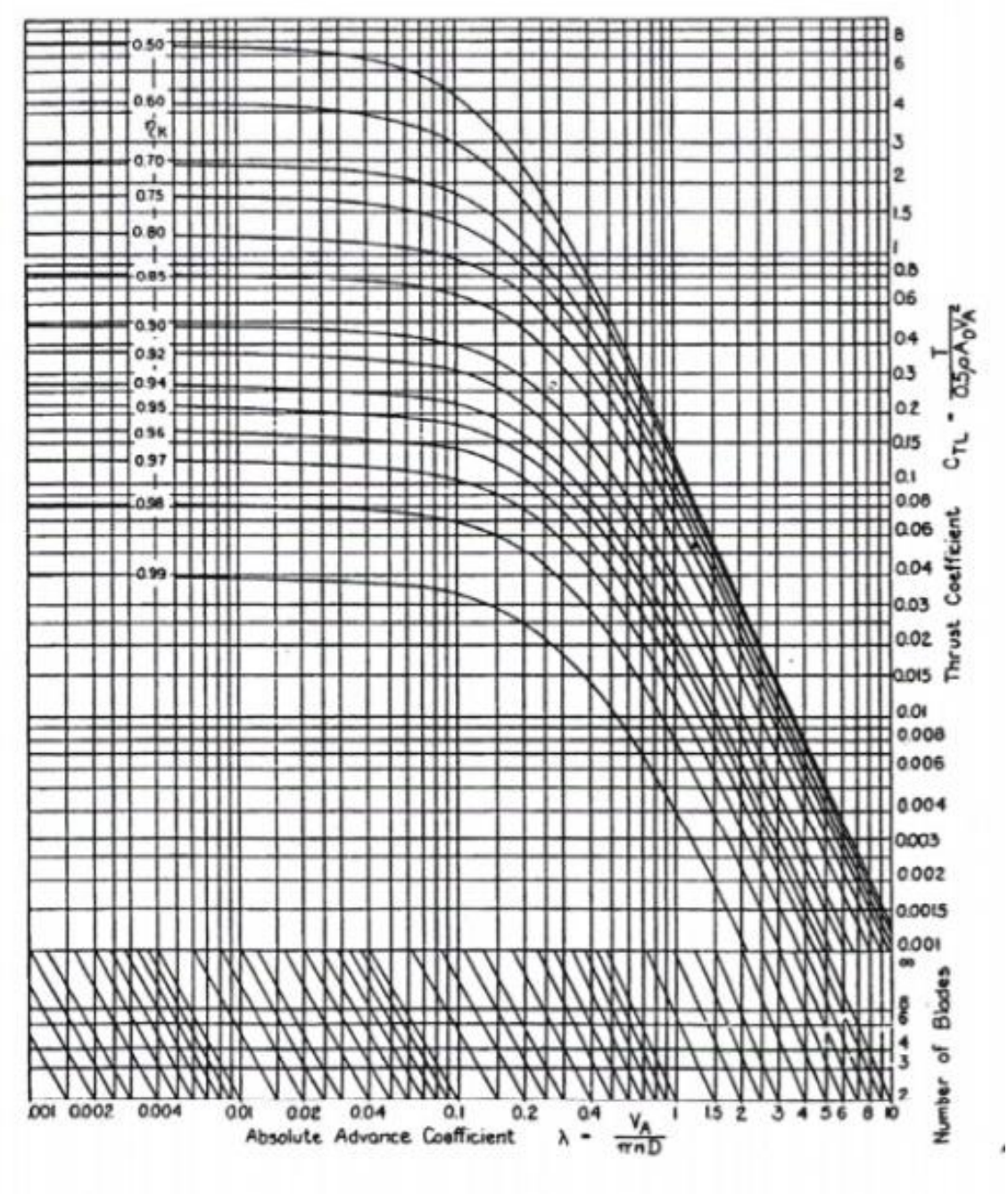

## APPENDIX II

Standard Shaft diameters (inches)

| $D$ | $D_3$ | $D$ | $D_3$ | $D$ | $D_3$ |
|---|---|---|---|---|---|
| 1 | 1.00 | 5 | 125.0 | 9 | 729 |
| $1\frac{1}{4}$ | 1.95 | $5\frac{1}{4}$ | 145 | $9\frac{1}{2}$ | 857 |
| $1\frac{1}{2}$ | 3.38 | $5\frac{1}{2}$ | 166.4 | 10 | 1000 |
| $1\frac{3}{4}$ | 5.36 | $5\frac{3}{4}$ | 190.1 | $10\frac{1}{2}$ | 1157 |
| 2 | 8.00 | 6 | 216 | 11 | 1331 |
| $2\frac{1}{4}$ | 11.39 | $6\frac{1}{4}$ | 244 | $11\frac{1}{2}$ | 1520 |
| $2\frac{1}{2}$ | 15.63 | $6\frac{1}{2}$ | 275 | 12 | 1728 |
| $2\frac{3}{4}$ | 20.80 | $6\frac{3}{4}$ | 308 | $12\frac{1}{2}$ | 1953 |
| 3 | 27.00 | 7 | 343 | 13 | 2197 |
| $3\frac{1}{4}$ | 34.33 | $7\frac{1}{4}$ | 381 | 14 | 2744 |
| $3\frac{1}{2}$ | 42.88 | $7\frac{1}{2}$ | 422 | 15 | 3375 |
| $3\frac{3}{4}$ | 52.73 | $7\frac{3}{4}$ | 465 | 16 | 4096 |
| 4 | 64.00 | 8 | 512 | 17 | 4913 |
| $4\frac{1}{4}$ | 76.77 | $8\frac{1}{4}$ | 562 | 18 | 5832 |
| $4\frac{1}{2}$ | 91.13 | $8\frac{1}{2}$ | 614 | 19 | 6859 |
| $4\frac{3}{4}$ | 107.2 | $8\frac{3}{4}$ | 670 | 20 | 8000 |

Source: The Falk Corporation (www.sciencedirect.com)

## APPENDIX III

The technical drawing of the 4-bladed propeller

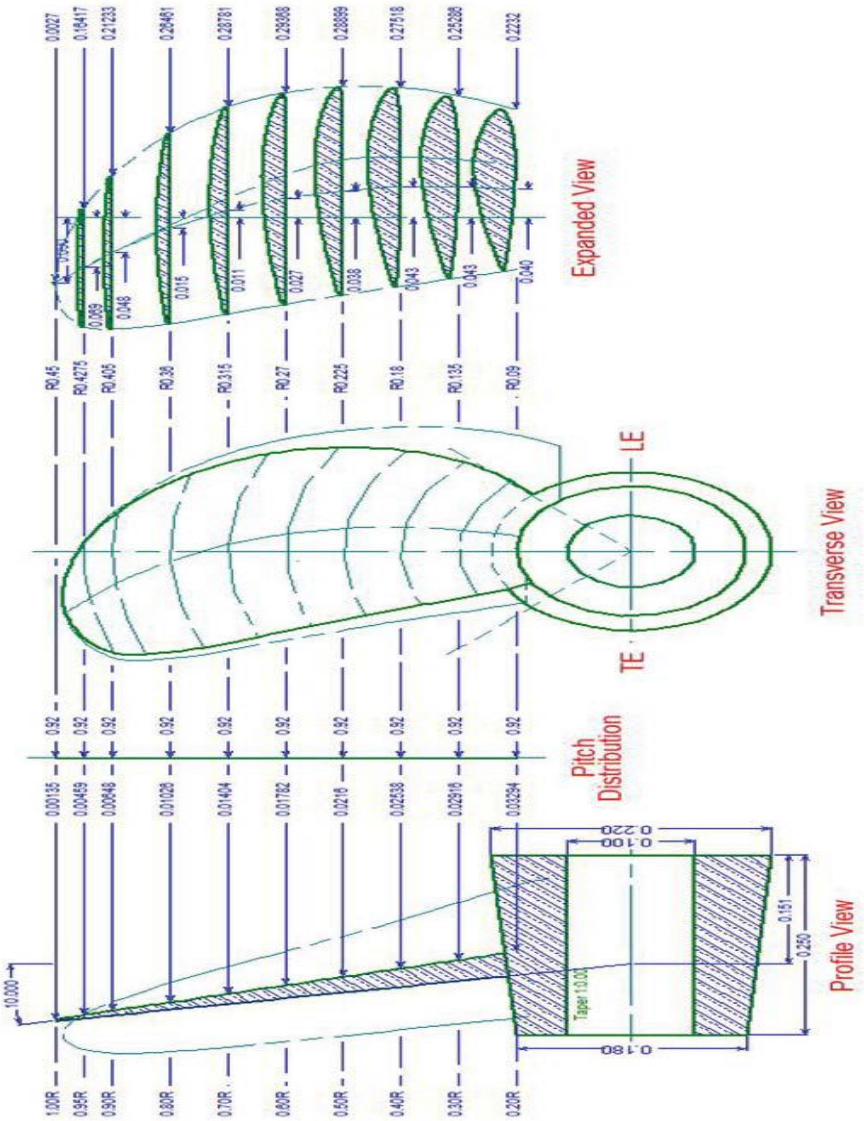

## APPENDIX IV

Standard Materials Classified by Lloyd's Register of Shipping.

| **MATERIALS** | **S.I UNITS** | | | **METRIC UNITS** | | |
|---|---|---|---|---|---|---|
| | Specified Minimum Tensile Strength | G Density | U Allowable Stress | Specified Minimum Tensile Strength | G Density | U Allowable Stress |
| Gray cast iron Spherical or modular | 250 | 7.2 | 17.2 | 25 | 7.2 | 17.5 |
| graphite cast iron | 400 | 7.3 | 20.6 | 41 | 7.3 | 2.1 |
| log alloy steels | 400 | 7.9 | 20.6 | 45 | 7.9 | 2.1 |
| carbon steels | 400 | 7.9 | 20.6 | 41 | 7.9 | 2.1 |
| 13% chromium stainless steels | 540 | 7.7 | 41 | 55 | 7.7 | 42 |
| Chromium-Nickel authentic stainless steel | 540 | 7.6 | 41 | 46 | 7.9 | 4.2 |
| Grade Cu1, manganese Bonze (higher tensile brass) | 440 | 8.3 | 39 | 45 | 8.3 | 4 |
| Grade Cu3 Nickel, Aluminum Bronze | 590 | 7.6 | 56 | 60 | 7.6 | 5.7 |
| Grade Cu4, Manganese Aluminum Bronze | 630 | 7.5 | 4.6 | 64 | 7.5 | 4.7 |

## APPENDIX V

$B_p$ Chart series 4.55

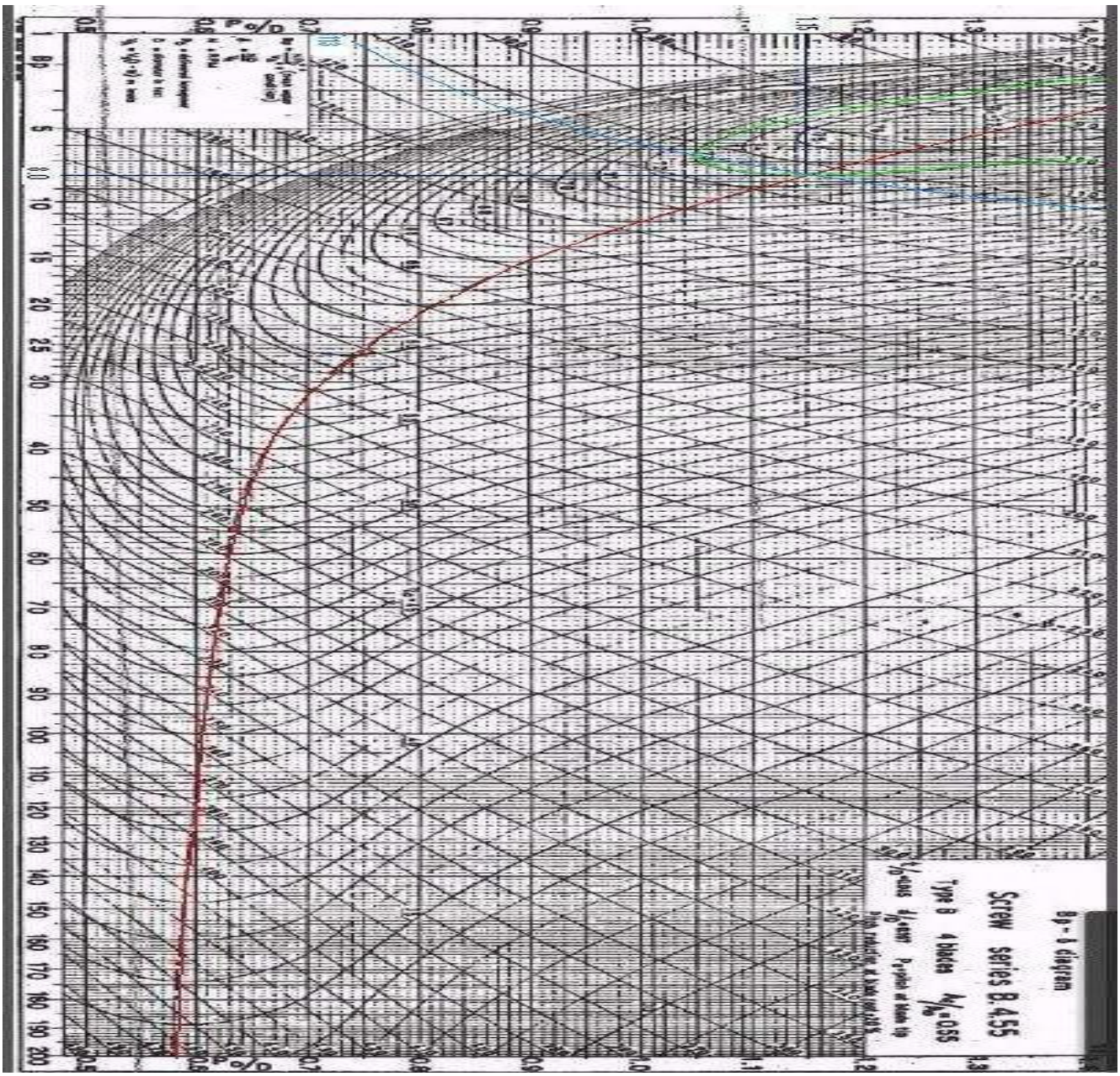

# APPENDIX VI
# SOLIDWORKS SIMULATION RESULTS OF PROPELLER BLADE STATIC AND FLOW ANALYSIS

| *Column1* | *Column2* | *Column3* | *Column4* | *Column5* | *Column6* | *Column7* | *Column8* | *Column9* | *Column10* |
|---|---|---|---|---|---|---|---|---|---|
| | | | | | | | | | |
| *DS(m E+02)* | *rB (m)* | *Ms(kg)* | *MTB (kg)* | *Load imposed by combined mass (N)* | *MAXSS (N/m^2)* | *MSS (N/m^2)* | *RRP rad/s* | *App. RPM* | *Nos. of Blades* |
| *0.135* | *0.3* | *5.66E+06* | *2.87E+05* | *1,200.00* | *2.49E+05* | *9.05E+01* | *49.7783* | *475* | *3* |
| | | | | | | | | | |
| *DS(m E+02)* | *rB (m)* | *Ms(kg)* | *MTB (kg)* | *Load Produced by Engine RPM (N)* | *MAXSS (N/m^2)* | *MSS (N/m^2)* | *Engine rad/s* | *App. RPM* | *Nos. of Blades* |
| *0.135* | *0.3* | *5.66E+06* | *2.87E+05* | *6,116.55* | *1.27E+06* | *4.61E+02* | *62.831* | *600* | *3* |
| | | | | | | | | | |
| *DS(m E+02)* | *rB (m)* | *Ms(kg)* | *MTB (kg)* | *LCM (N)* | *MAXSS (N/m^2)* | *MSS (N/m^2)* | *RRP rad/s* | *App. RPM* | *Nos. of Blades* |
| *0.135* | *0.3* | *5.66E+06* | *2.87E+05* | *1,200.00* | *2.49E+05* | *9.05E+01* | *49.018* | *468.1* | *4* |
| | | | | | | | | | |
| *DS(m E+02)* | *rB (m)* | *Ms(kg)* | *MTB (kg)* | *LPE (N)* | *MAXSS (N/m^2)* | *MSS (N/m^2)* | *Engine rad/s* | *App. RPM* | *Nos. of Blades* |
| *0.135* | *0.3* | *5.66E+06* | *2.87E+05* | *7,417.74* | *1.54E+06* | *5.60E+02* | *62.831* | *600* | *4* |
| | | | | | | | | | |
| *Material Yield Stress (N/m^2) : 5.30E+08* | | | | | | | | | |
| *Engine RPM : 600* | | | | | | | | | |
| *Alternate Models linking Propeller rad/s to Force Produced* | | | | | | | | | |
| *y = 376.67x - 17550* | *Used (Ref: Parametric Stud. 1_3 Blades)* | | | | | | | | |
| *y = 368.45x - 16334* | *(Ref: Parametric Stud. 1_4 Blades)* | | | | | | | | |
| *y = 450.14x - 20865* | *Used (Ref: Parametric Stud. 1_5 Blades)* | | | | | | | | |
| | | | | | | | | | |
| *Formula for imposed load by a recognized singular particle: F(i) = [(m(1)-m(2))*a+V)* | | | | | | | | | |
| *Combined imposed load from all recognized particles simply has an additive relationship: F(t)= F(1)+F(2)* | | | | | | | | | |
| *Upthrust (U) = m(1)g-V* | | | | | | | | | |
| *Counter-balanced mass (m(2))= U/g* | | | | | | | | | |
| *Total mass of Singular particle (m(1))* | | | | | | | | | |
| *Assumed Viscous effect (V) = 500N* | | | | | | | | | |
| *Acceleration of Particle (a) = 2m/s^2* | | | | | | | | | |
| *Accelaration due to gravity (g) = 10m/s^2* | | | | | | | | | |
| *N/B: All particles are assumed to have uniform and identical acceleration.* | | | | | | | | | |

# APPENDIX VII

## SOLIDWORKS SIMULATION RESULTS OF PROPELLER BLADE STATIC AND FLOW ANALYSIS (MORE DETAILED)

**Load imposed by combined mass(LCM)  Load Produced by Engine(LPE)**

| Column5 | Column6 | Column7 | Column8 | Column9 | Column10 |
|---|---|---|---|---|---|
| LCM (N) | MAXSS (N/m^2) | MINSS (N/m^2) | RRP rad/s | App. RPM | Nos. of Blades |
| 1,200.00 | 2.49E+05 | 9.05E+01 | 49.7783 | 475 | 3 |
| | | | | | |
| LPE RPM (N) | MAXSS (N/m^2) | MSS (N/m^2) | Engine rad/s | App. RPM | Nos. of Blades |
| 6,116.55 | 1.27E+06 | 4.61E+02 | 62.831 | 600 | 3 |
| | | | | | |
| LCM (N) | MAXSS (N/m^2) | MSS (N/m^2) | RRP rad/s | App. RPM | Nos. of Blades |
| 1,200.00 | 2.49E+05 | 9.05E+01 | 49.018 | 468.1 | 4 |
| | | | | | |
| LPE (N) | MAXSS (N/m^2) | MSS (N/m^2) | Engine rad/s | App. RPM | Nos. of Blades |
| 7,417.74 | 1.54E+06 | 5.60E+02 | 62.831 | 600 | 4 |
| | | | | | |
| LCM (N) | MAXSS (N/m^2) | MSS (N/m^2) | RRP rad/s | App. RPM | Nos. of Blades |
| 1,200.00 | 2.49E+05 | 9.05E+01 | 48.258 | 461.2 | 5 |
| | | | | | |
| LPE RPM (N) | MAXSS (N/m^2) | MSS (N/m^2) | Engine rad/s | App. RPM | Nos. of Blades |
| 6,116.55 | 1.81E+06 | 6.59E+02 | 62.831 | 600 | 5 |
| | | | | | |
| LCM (N) | MAXSS (N/m^2) | MSS (N/m^2) | RRP rad/s | App. RPM | Nos. of Blades |
| 1,200.00 | 2.49E+05 | 9.05E+01 | 47.497 | 454.3 | 6 |
| | | | | | |
| LPE (N) | MAXSS (N/m^2) | MSS (N/m^2) | Engine rad/s | App. RPM | Nos. of Blades |
| 7,417.74 | 2.08E+06 | 7.58E+02 | 62.831 | 600 | 6 |